The Alk receptor tyrosine kinase regulates Sparkly, a novel activity regulating neuropeptide precursor in the *Drosophila* CNS

Sanjay Kumar Sukumar, Vimala Antonydhason, Linnea Molander, Jawdat Sandakly, Malak Kleit, Ganesh Umapathy, Patricia Mendoza-Garcia, Tafheem Masudi, Andreas Schlossser, Dick R. Nässel, Christian Wegener, Margret Shirinian, Ruth H. Palmer ✉

Department of Medical Biochemistry and Cell Biology, Institute of Biomedicine, University of Gothenburg, SE-405 30 Gothenburg, Sweden • Department of Experimental Pathology, Immunology and Microbiology, Faculty of Medicine, American University of Beirut, Beirut 1107 2020, Lebanon • Julius-Maximilians-Universität Würzburg, Rudolf-Virchow-Center, Center for Integrative and Translational Bioimaging, 97080 Würzburg, Germany • Department of Zoology, Stockholm University, SE-106 91 Stockholm, Sweden • Julius-Maximilians-Universität Würzburg, Biocenter, Theodor-Boveri-Institute, Neurobiology and Genetics, 97074 Würzburg, Germany

Abstract

Numerous roles for the Alk receptor tyrosine kinase have been described in *Drosophila*, including functions in the central nervous system (CNS), however the molecular details are poorly understood. To gain mechanistic insight, we employed Targeted DamID (TaDa) transcriptional profiling to identify targets of Alk signaling in the larval CNS. TaDa was employed in larval CNS tissues, while genetically manipulating Alk signaling output. The resulting TaDa data were analysed together with larval CNS scRNA-seq datasets performed under similar conditions, identifying a role for Alk in the transcriptional regulation of neuroendocrine gene expression. Further integration with bulk/scRNA-seq and protein datasets from larval brains in which Alk signaling was manipulated, identified a previously uncharacterized *Drosophila* neuropeptide precursor encoded by *CG4577* as an Alk signaling transcriptional target. *CG4577*, which we named *Sparkly (Spar)*, is expressed in a subset of Alk-positive neuroendocrine cells in the developing larval CNS, including circadian clock neurons. In agreement with our TaDa analysis, overexpression of the *Drosophila* Alk ligand Jeb resulted in increased levels of Spar protein in the larval CNS. We show that Spar protein is expressed in circadian (Clock) neurons, and flies lacking Spar exhibit defects in sleep and circadian activity control. In summary, we report a novel activity regulating neuropeptide precursor gene that is regulated by Alk signaling in the *Drosophila* CNS.

eLife assessment

Receptor tyrosine kinases such as ALK play critical roles during appropriate development and behaviour and are nodal in many disease conditions, through molecular mechanisms that weren't completely understood. This manuscript identifies a previously unknown neuropeptide precursor as a downstream transcriptional target of Alk signalling in Clock neurons in the Drosophila brain. The experiments are well designed with attention to detail, the data are **solid**, and the findings will be **useful** to those interested in events downstream of signalling by receptor tyrosine kinases.

Introduction

Receptor tyrosine kinases (RTK) are involved in wide range of developmental processes. In humans, the Anaplastic Lymphoma Kinase (ALK) RTK is expressed in the central and peripheral nervous system and its role as an oncogene in the childhood cancer neuroblastoma, which arises from the peripheral nervous system, is well described (Iwahara *et al*, 1997 ; Matthay *et al*, 2016 ; Umapathy *et al*, 2019 ; Vernersson *et al*, 2006).

In *Drosophila melanogaster,* Alk is expressed in the visceral mesoderm, central nervous system (CNS) and at neuromuscular junctions (NMJ). The critical role of *Drosophila* Alk and its ligand Jelly belly (Jeb) in the development of the embryonic visceral mesoderm has been extensively studied (Englund *et al*, 2003 ; Jin *et al*, 2013 ; Lee *et al*, 2003 ; Loren *et al*, 2003 ; Mendoza-Garcia *et al*, 2021 ; Mendoza-Garcia *et al*, 2017 ; Pfeifer *et al*, 2022 ; Popichenko *et al*, 2013 ; Reim *et al*, 2012 ; Schaub & Frasch, 2013 ; Shirinian *et al*, 2007 ; Stute *et al*, 2004 ; Varshney & Palmer, 2006 ; Wolfstetter *et al*, 2017). In the CNS, Alk signaling has been implicated in diverse functions, including targeting of photoreceptor axons in the developing optic lobes (Bazigou *et al*, 2007), regulation of NMJ synaptogenesis and architecture (Rohrbough & Broadie, 2010 ; Rohrbough *et al*, 2013) and mushroom body neuronal differentiation (Pfeifer *et al*., 2022). In addition, roles for Alk in neuronal regulation of growth and metabolism, organ sparing and proliferation of neuroblast clones, as well as sleep and long-term memory formation in the CNS have been reported (Bai & Sehgal, 2015 ; Cheng *et al*, 2011 ; Gouzi *et al*, 2011 ; Orthofer *et al*, 2020). The molecular mechanisms underlying these Alk-driven phenotypes are currently under investigation, with some molecular components of *Drosophila* Alk signaling in the larval CNS, such as the protein tyrosine phosphatase Corkscrew (Csw), identified in recent BioID-based *in vivo* proximity labeling analyses (Uckun *et al*, 2021).

In this work, we aimed to capture Alk-signaling dependent transcriptional events in the *Drosophila* larval CNS using Targeted DamID (TaDa) that profiles RNA polymerase II (Pol II) occupancy. TaDa employs a prokaryotic DNA adenine methyltransferase (Dam) to specifically methylate adenines within GATC sequences present in the genome, creating unique GA^{me}TC marks. In TaDa, expression of Dam fused to Pol II results in GA^{me}TC marks on sequences adjacent to the Pol II binding site and can be combined with the Gal4/UAS system to achieve cell-type specific transcriptional profiling (Southall *et al*, 2013). Tissue specific TaDa analysis of Alk signaling, while genetically manipulating Alk signaling output, has previously been used to identify Alk transcriptional targets in the embryonic visceral mesoderm, such as the transcriptional regulator *Kahuli (Kah)* (Mendoza-Garcia *et al*., 2021). Here, we employed this strategy to identify Alk transcriptional targets in *Drosophila* larval brain tissue. These Alk TaDa identified transcripts were enriched in neuroendocrine cells. Further integration with bulk RNA-seq datasets generated from *Alk* gain-of-function and loss-of-function alleles, identified the

uncharacterized neuropeptide precursor (*CG4577*), as an Alk target in the *Drosophila* brain, that we have named *Sparkly (Spar)* based on its protein expression pattern. Spar is expressed in a subset of Alk-expressing cells in the central brain and ventral nerve cord, overlapping with the expression pattern of neuroendocrine specific transcription factor Dimmed (Dimm) (Hewes *et al,* 2003). Further, using genetic manipulation of Alk we show that Spar levels in the CNS respond to Alk signaling output, validating *Spar* as a transcriptional target of Alk. *Spar* mutant flies showed significant reduction in life-span, and behavioral phenotypes including defects in activity, sleep, and circadian activity.

Notably, *Alk* loss-of-function alleles displayed similar behavioral defects, suggesting that Alk-dependant regulation of Spar in peptidergic neuroendocrine cells modulates activity and sleep/rest behavior. Interestingly, Alk and its ligand Alkal2 play a role in regulation of behavioral and neuroendocrine function in vertebrates (Ahmed *et al*, 2022 ; Bilsland *et al*, 2008 ; Borenas *et al*, 2021 ; Lasek *et al*, 2011a ; Lasek *et al*, 2011b ; Orthofer *et al.,* 2020 ; Weiss *et al*, 2012 ; Witek *et al*, 2015). Taken together, our findings suggest an evolutionarily conserved role of Alk signaling in the regulation of neuroendocrine cell function and identify *Spar* as the first molecular target of Alk to be described in the regulation of activity and circadian control in the fly.

Results

TaDa identifies Alk-regulated genes in *Drosophila* larval CNS

To characterize Alk transcriptional targets in the *Drosophila* CNS we employed Targeted DamID (TaDa). Briefly, transgenic DNA adenine methyltransferase (Dam) fused with RNA-Pol II (here after referred as Dam-Pol II) (Southall *et al.,* 2013) **(Figure 1a-b)**, was driven using the pan neuronal *C155-Gal4* driver. To inhibit Alk signaling we employed a dominant negative Alk transgene, which encodes the Alk extracellular and transmembrane domain (here after referred as *UAS-Alk^{DN}*) (Bazigou *et al.,* 2007) **(Figure 1a)**. Flies expressing Dam-Pol II alone in a wild-type background were used as control. Expression of Dam-Pol II was confirmed by expression of mCherry, which is encoded by the primary ORF of the TaDa construct (Southall *et al.,* 2013) **(Figure 1b , Figure 1 – figure supplement 1a-b')**. CNS from third instar wandering larvae were dissected and genomic DNA was extracted, fragmented at GA^{me}TC marked sites using methylation specific DpnI restriction endonuclease. The resulting GATC fragments were subsequently amplified for library preparation and NGS sequencing **(Figure 1 – figure supplement 1c)**. Bioinformatic data analysis was performed based on a previously described pipeline (Marshall & Brand, 2017 ; Mendoza-Garcia *et al.,* 2021). Initial quality control analysis indicated comparable numbers of quality reads between samples and replicates, identifying >20 million raw reads per sample that aligned to the *Drosophila* genome **(Figure 1 – figure supplement 1d-d')**. No significant inter-replicate variability was observed **(Figure 1 – figure supplement 1e)**. Meta-analysis of reads associated with GATC borders showed a tendency to accumulate close to Transcription Start Sites (TSS) indicating the ability of TaDa to detect transcriptionally active regions **(Figure 1 – figure supplement 1f)**. A closer look at the Pol II occupancy profile of *Alk* shows a clear increase in Pol II occupancy from Exon 1 to Exon 7 (encoding the extracellular and transmembrane domain) in *Alk^{DN}* samples reflecting the expression of the dominant negative *Alk* transgene **(Figure 1 – figure supplement 1g)**.

To detect differential Pol II occupancy between Dam-Pol II control (*C155-Gal4>UAS-LT3-Dam::Pol ll*) and *UAS-Alk^{DN}* (*C155-Gal4>UAS-LT3-Dam::Pol II; UAS-Alk^{DN}*) samples, neighbouring GATC associated reads, maximum 350 bp apart (median GATC fragment distance in the *Drosophila* genome) were clustered in peaks (Tosti *et al*, 2018). More than 10 million reads in both control and *Alk^{DN}* samples were identified as GATC associated reads **(Figure 1 – figure supplement 1d')**,
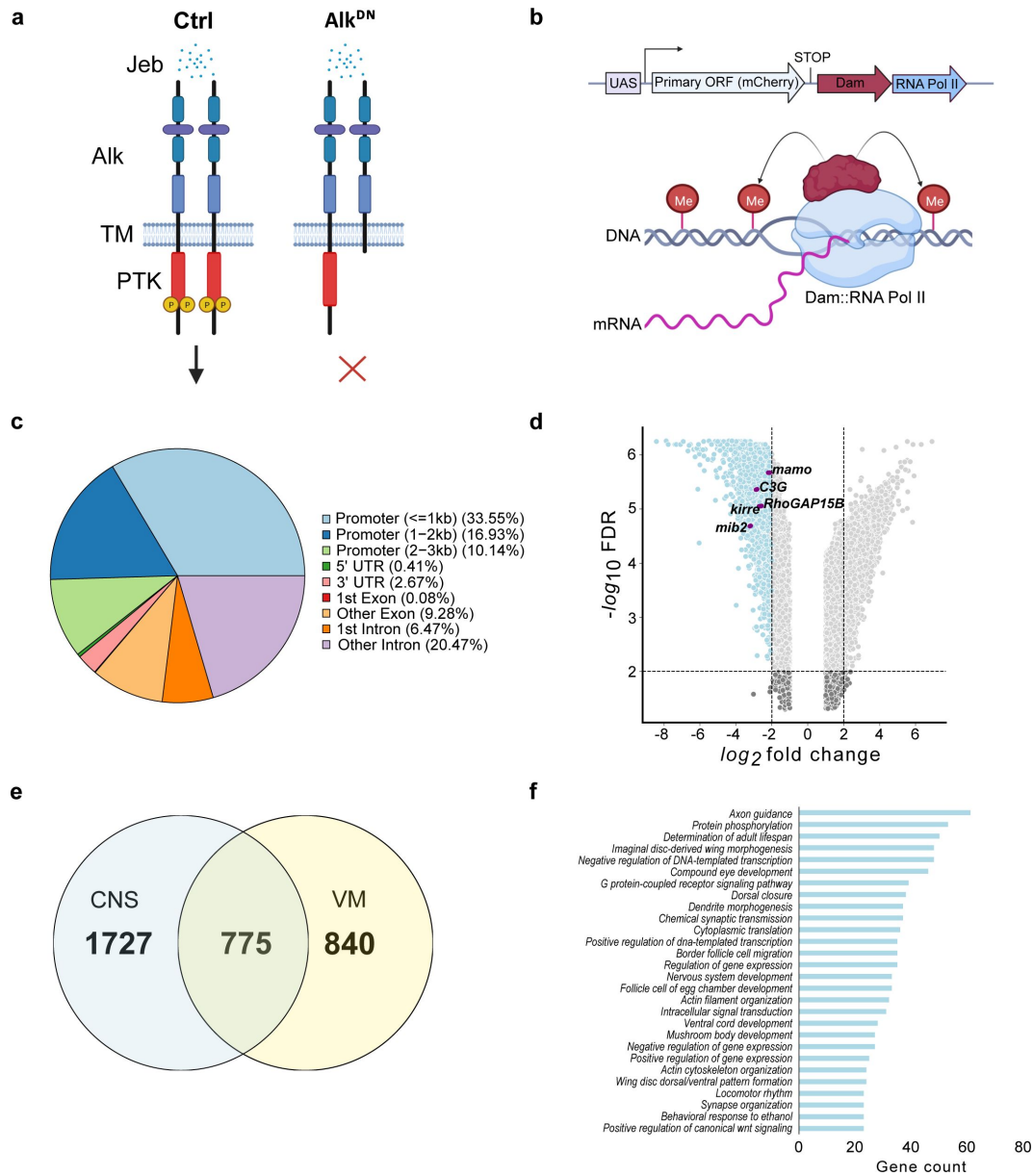
Figure 1.

TaDa-seq identifies novel Alk-regulated genes in the *Drosophila* larval CNS.

a. Schematic overview of experimental conditions comparing wild-type Alk (Ctrl) with Alk dominant-negative (*Alk^{DN}*) conditions. The *Drosophila* Alk RTK is comprised of extracellular, transmembrane and intracellular kinase (red) domains. Upon Jelly belly (Jeb, blue dots) ligand stimulation the Alk kinase domain is auto-phosphorylated (yellow circles) and downstream signaling is initiated. In *Alk^{DN}* experimental conditions, Alk signaling is inhibited due to overexpression of the Alk extracellular domain. **b.** The TaDa system (expressing *Dam::RNA Pol II*) leads to the methylation of GATC sites in the genome, allowing transcriptional profiling based on RNA Pol II occupancy. **c.** Pie chart indicating the distribution of TaDa peaks on various genomic features such as promoters, 5' UTRs, 3' UTRs, exons and introns. **d.** Volcano plot of TaDa-positive loci enriched in *Alk^{DN}* experimental conditions compared to control loci exhibiting Log2FC<-2, *p*≥0.05 are shown in blue. Alk-associated genes such as *mamo, C3G, Kirre, RhoGAP15B* and *mib2* are highlighted in purple. **e.** Venn diagram indicating Alk-dependant TaDa downregulated genes from the current study compared with previously identified Alk-dependant TaDa loci in the embryonic VM (Mendoza-Garcia *et al*., 2021 ⧉). **f.** Enrichment of Gene Ontology (GO) terms associated with significantly down-regulated genes in *Alk^{DN}* experimental conditions.

and those loci displaying differential Pol II occupancy were defined by logFC and FDR (as detailed in materials and methods). Greater than 50% of aligned reads were in promoter regions, with 33.55% within a 1 kb range **(Figure 1c ⧉, Table S1)**.

To further analyse transcriptional targets of Alk signaling we focused on loci exhibiting decreased Pol II occupancy when compared with controls, identifying 2502 loci with logFC<-2, FDR<0.05 **(Figure 1d ⧉, Table S1)**. Genes previously known to be associated with Alk signaling, such as *kirre*, *RhoGAP15B*, *C3G*, *mib2* and *mamo*, were identified among downregulated loci **(Figure 1d ⧉)**. We compared CNS TaDa Alk targets with our previously published embryonic visceral mesoderm TaDa datasets that were derived under similar experimental conditions (Mendoza-Garcia *et al.,* 2021 ⧉) and found 775 common genes **(Figure 1e ⧉, Table S1)**. Gene ontology (GO) analysis identified GO terms in agreement with previously reported Alk functions in the CNS (Bai & Sehgal, 2015 ⧉; Bazigou *et al.,* 2007 ⧉; Cheng *et al.,* 2011 ⧉; Gouzi *et al.,* 2011 ⧉; Orthofer *et al.,* 2020 ⧉; Pfeifer *et al.,* 2022 ⧉; Rohrbough & Broadie, 2010 ⧉; Rohrbough *et al.,* 2013 ⧉; Woodling *et al,* 2020 ⧉) such as axon guidance, determination of adult lifespan, nervous system development, regulation of gene expression, mushroom body development, behavioral response to ethanol and locomotor rhythm (**Figure 1f ⧉**). Many of the differentially regulated identified loci have not previously been associated with Alk signaling and represent candidates for future characterisation.

TaDa targets are enriched for neuroendocrine transcripts

To further characterize Alk-regulated TaDa loci, we set out to examine their expression in scRNA-seq data from wild-type third instar larval CNS (Pfeifer *et al.,* 2022 ⧉). Enrichment of TaDa loci were identified by using AUCell, an area-under-the-curve based enrichment score method, employing the top 500 TaDa hits (Aibar *et al,* 2017 ⧉) **(Figure 2a-b ⧉, Table S1)**. This analysis identified 786 cells (out of 3598), mainly located in a distinct cluster of mature neurons that robustly express both *Alk* and *jeb* **(Figure 2b ⧉, red circle; Figure 2c ⧉)**. This cluster was defined as neuroendocrine cells based on canonical markers, such as the neuropeptides *Lk* (*Leucokinin*), *Nplp1* (*Neuropeptide-like precursor 1*), *Dh44* (*Diuretic hormone 44*), *Dh31* (*Diuretic hormone 31*), *sNPF* (*short neuropeptide F*), *AstA* (*Allatostatin A*), and the enzyme *Pal2* (*Peptidyl-α-hydroxyglycine-α-amidating lyase 2*) as well as *Eip74EF* (*Ecdysone-induced protein 74EF*), and *Rdl* (resistance to dieldrin) (Guo *et al,* 2019 ⧉; Huckesfeld *et al,* 2021 ⧉; Takeda & Suzuki, 2022 ⧉; Torii, 2009 ⧉) **(Figure 2d-f ⧉)**. Overall, the TaDa-scRNAseq data integration analysis suggests a role of Alk signaling in regulation of gene expression in neuroendocrine cells.

To further explore the observed enrichment of Alk-regulated TaDa loci in neuroendocrine cells, we used a Dimmed (Dimm) transcription factor reporter (*Dimm-Gal4>UAS-GFPcaax*), as a neuroendocrine marker (Park *et al,* 2008 ⧉), to confirm Alk protein expression in a subset of neuroendocrine cells in the larval central brain, ventral nerve cord and neuroendocrine corpora cardiaca cells **(Figure 2g ⧉, Figure 2 – figure supplement 1)**. This could not be confirmed at the RNA level, due to low expression of *dimm* in both our and publicly available single cell RNASeq datasets (Brunet Avalos *et al,* 2019 ⧉; Michki *et al,* 2021 ⧉; Pfeifer *et al.,* 2022 ⧉).

Multi-omics integration identifies *CG4577* as an Alk transcriptional target

Loci potentially subject to Alk-dependent transcriptional regulation were further refined by integration of the Alk-regulated TaDa dataset with previously collected RNA-seq datasets **(Figure 3a ⧉)**. Specifically, w^{1118} (control), Alk^{Y1355S} (Alk gain-of-function) and $Alk^{\Delta RA}$ (Alk loss-of-function) RNA-seq datasets (Pfeifer *et al.,* 2022 ⧉) were compared to identify genes that exhibited both significantly increased expression in Alk gain-of-function conditions (w^{1118} vs Alk^{Y1355S}) and significantly decreased expression in Alk loss-of-function conditions (w^{1118} vs $Alk^{\Delta RA}$ and control vs *C155-Gal4* driven expression *of UAS-Alk*^{DN}). Finally, we positively selected for candidates expressed in *Alk*-positive cells in our scRNA-seq dataset. Notably, the only candidate which met
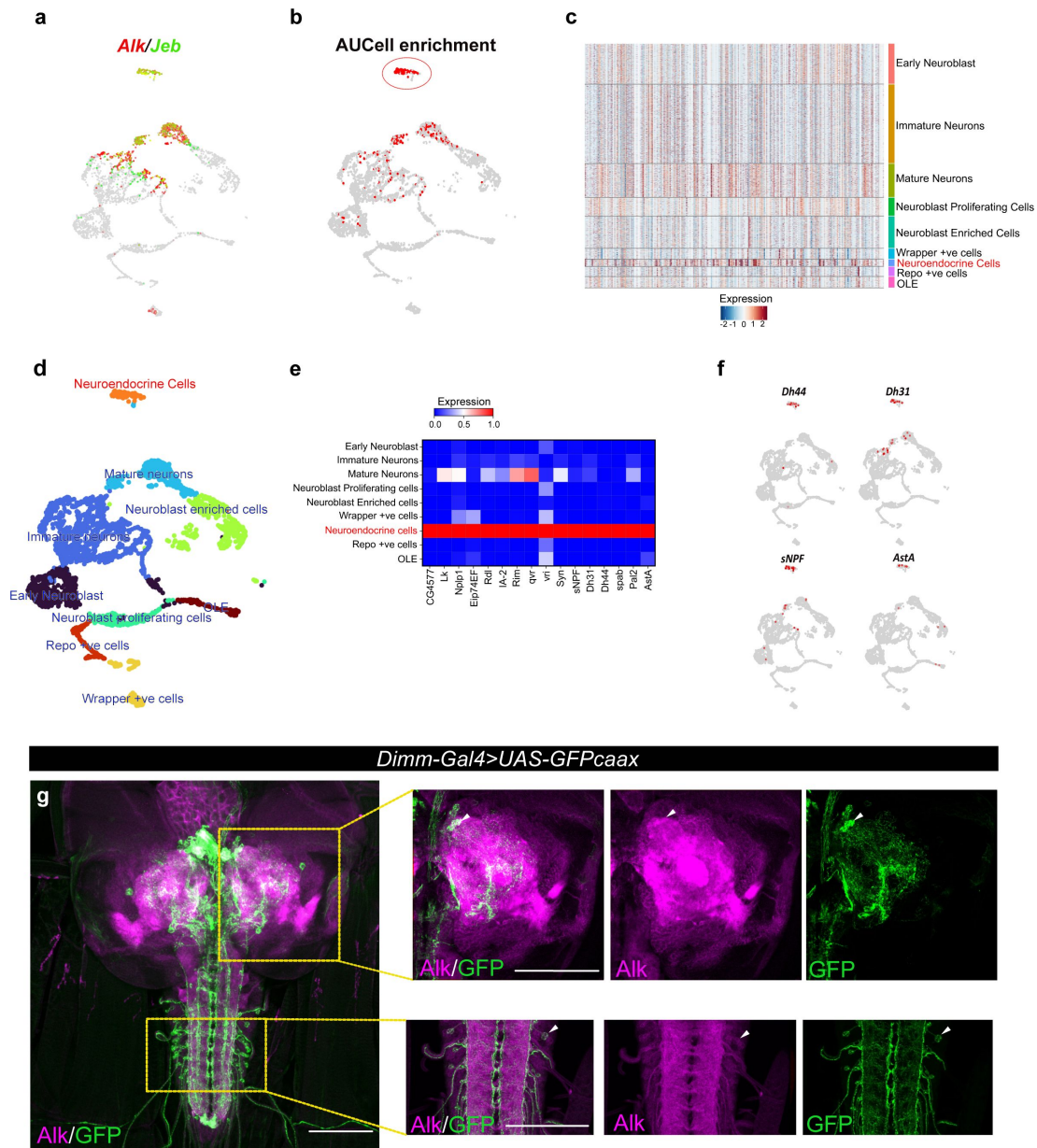
Figure 2.

Integration of TaDa data with scRNA-seq identifies an enrichment of Alk-regulated genes in neuroendocrine cells.

a. UMAP feature plot indicating Alk (in red) and Jeb (in green) mRNA expression in a control (w^{1118}) whole third instar larval CNS scRNA-seq dataset (Pfeifer *et al.*, 2022 ⤢). **b.** UMAP visualizing AUCell enrichment analysis of the top 500 TaDa downregulated genes in the third instar larval CNS scRNA-seq dataset. Cells exhibiting an enrichment (threshold >0.196) are depicted in red. One highly enriched cell cluster is highlighted (red circle). **c.** Heatmap representing expression of the top 500 genes downregulated in TaDa Alk^{DN} samples across larval CNS scRNA-seq clusters identifies enrichment in neuroendocrine cells. **d.** UMAP indicating third instar larval CNS annotated clusters (Pfeifer *et al.*, 2022 ⤢), including the annotated neuroendocrine cell cluster (in orange). **e.** Matrix plot displaying expression of canonical neuroendocrine cell markers. **f.** Feature plot visualizing mRNA expression of *Dh44*, *Dh31*, *sNPF* and *AstA* neuropeptides across the scRNA population. **g.** Alk staining in *Dimm-Gal4>UAS-GFPcaax* third instar larval CNS confirms Alk expression in Dimm-positive cells. Alk (in magenta) and GFP (in green), close-ups indicated by boxed regions and arrows indicating overlapping cells in the central brain and ventral nerve cord. Scale bars: 100 μm.

these stringent criteria was *CG4577*, which encodes an uncharacterized putative neuropeptide precursor (**Figure 3b**). *CG4577* exhibited decreased Pol II occupancy in *Alk^{DN}* samples **(Figure 3c**), and *CG4577* transcripts were upregulated in *Alk^{Y1355S}* gain-of-function conditions and downregulated in *Alk^{ΔRA}* loss-of-function conditions (**Figure 3d** , **Table S1**). In agreement with a potential role as a neuropeptide precursor, expression of *CG4577* was almost exclusively restricted to neuroendocrine cell clusters in our scRNA-seq dataset (**Figure 3e**). Examination of additional publicly available first instar larval and adult CNS scRNAseq datasets (Brunet Avalos *et al.,* 2019 ; Davie *et al,* 2018) confirmed the expression of *CG4577* in Alk-expressing cells (**Figure 3** – **figure supplement 1a-b**). *CG4577-RA* encodes a 445 amino acid prepropeptide with a 27 aa N-terminal signal peptide sequence as predicted by SignalP-5.0 (**Figure 3f**) (Almagro Armenteros *et al,* 2019). Analysis of CG4577-PA at the amino acid level identified a high percentage of glutamine residues (43 of 445; 9%), including six tandem glutamine repeats (amino acids 48-56, 59-62, 64-71, 116-118, 120-122 and 148-150) of unknown function as well as a lack of cysteine residues. The preproprotein has an acidic pI of 5.1 and carries a net negative charge of 6. Several poly- and di-basic prohormone convertase (PC) cleavage sites were also predicted (KR, KK, RR, RK) (Pauls *et al,* 2014 ; Southey *et al,* 2006 ; Veenstra, 2000) **(Figure 3f**). Since the propeptide does not contain cysteine residues it is unable to form intracellular or dimeric disulfide bridges. A second transcript, *CG4577-RB*, encodes a 446 amino acid protein with only two amino acid changes **(Figure 3 – figure supplement 1c)**. Phylogenetic analysis of *CG4577* relative to known *Drosophila* neuropeptide precursors failed to identify strong homology in keeping with the known low sequence conservation of neuropeptide prepropeptides outside the bioactive peptide stretches. However, we were also unable to find sequence homologies with other known invertebrate or vertebrate peptides. Next, we searched for *CG4577* orthologs across Metazoa. We obtained orthologs across the Drosophilids, Brachyceran flies and Dipterans. No orthologs were found at higher taxonomic levels, suggesting that *CG4577* either originated in Dipterans, or has a high sequenc e variability at higher taxonomic levels. To identify conserved peptide stretches indicating putative bioactive peptide sequences, we aligned the predicted aa sequences of the Dipteran *CG4577* orthologs. This revealed several conserved peptide stretches (**Figure 3** – **figure supplement 2**) framed by canonical prohormone cleavage sites that might represent bioactive peptide sequences. BLAST searches against these conserved sequences did not yield hits outside of the Diptera.

CG4577/Spar is expressed in neuroendocrine cells

To further characterize *CG4577* we generated polyclonal antibodies that are predicted to recognize both CG4577-PA and CG4577-PB and investigated protein expression. CG4577 protein was expressed in a "sparkly" pattern in neurons of the third instar central brain as well as in distinct cell bodies and neuronal processes in the ventral nerve cord, prompting us to name CG4577 as Sparkly (Spar) (**Figure 4a-b**). Co-labeling of Spar and Alk confirmed expression of Spar in a subset of Alk-expressing cells, in agreement with our transcriptomics analyses (**Figure 4a** , **Figure 4** – **figure supplement 1**). In addition, we also observed expression of Spar in neuronal processes which emerge from the ventral nerve cord and appear to innervate larval body wall muscle number 8, that may be either Leukokinin (Lk) or cystine-knot glycoprotein hormone GPB5 expressing neurons **(Figure 4b**) (Cantera & Nässel, 1992 ; Sellami *et al,* 2011). Spar antibody specificity was confirmed in both *C155-Gal4>UAS-Spar-RNAi* larvae, where RNAi-mediated knock down of *Spar* resulted in loss of detectable signal (**Figure 4c-c** '), and in *C155-Gal4>UAS-Spar* larvae, exhibiting ectopic *Spar* expression in the larval CNS and photoreceptors of the eye disc (**Figure 4d-d** '). To further address Spar expression in the neuroendocrine system, we co-labelled with antibodies against Dimm to identify peptidergic neuronal somata (Allan et al., 2005) in a *Dimm-Gal4>UAS-GFPcaax* background. This further confirmed the expression of Spar in Dimm-positive peptidergic neuroendocrine cells in the larval CNS (**Figure 4e-e** '', **Figure 4** – **Movie supplements 1 and 2**). Moreover, co-staining of Spar and Dimm in the adult CNS showed similar results (**Figure 4** – **figure supplement 2**).
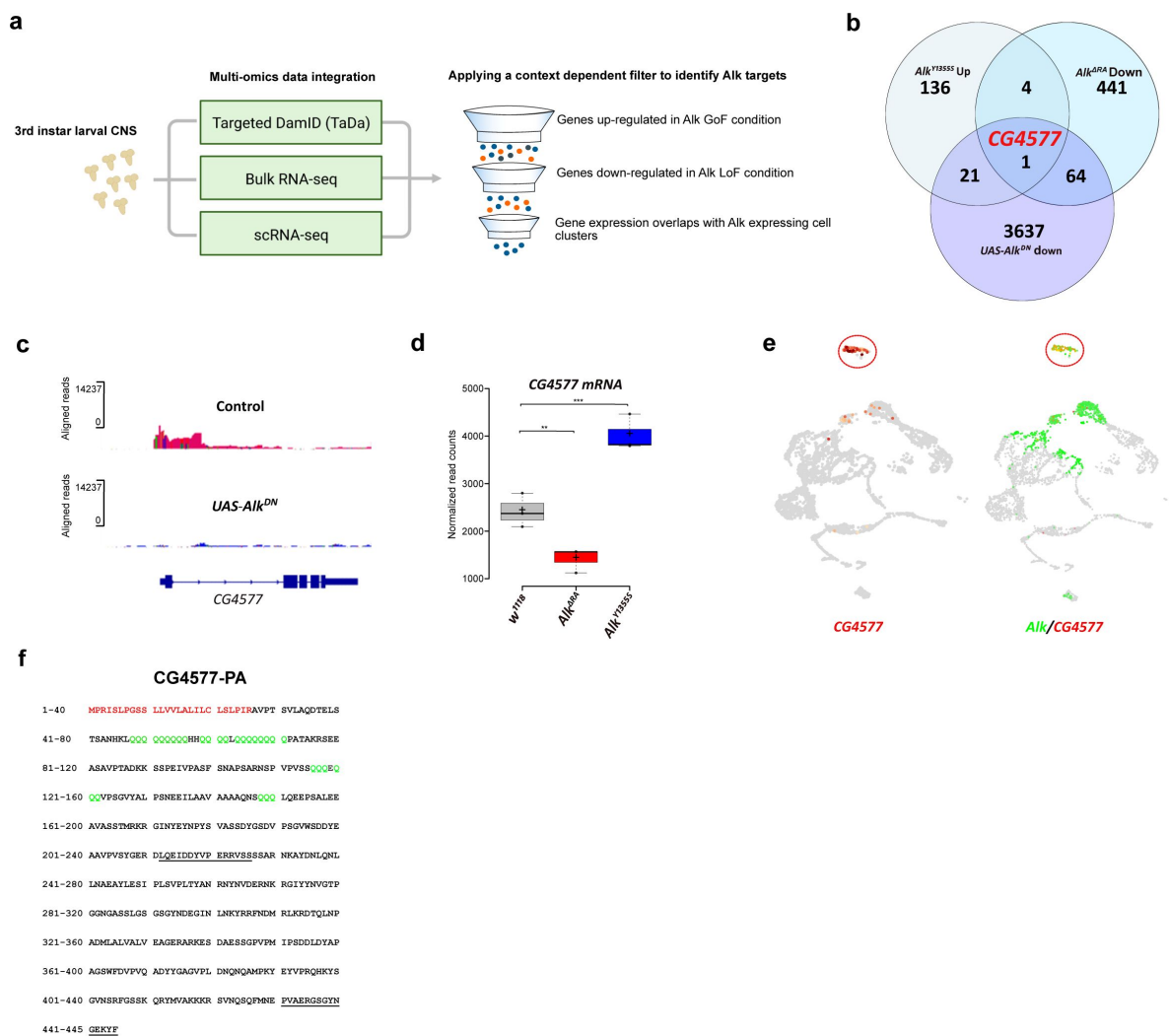
Figure 3.

TaDa and RNA-seq identifies CG4577 as a novel Alk-regulated neuropeptide.

a. Flowchart representation of the multi-omics approach employed in the study and the context dependent filter used to integrate TaDa, bulk RNA-seq and scRNA-seq datasets. **b.** Venn diagram comparing bulk RNA-seq (Log2FC>1.5, p<0.05) and TaDa datasets (Log2FC<-2, p<0.05). A single candidate (*CG4577/Spar*) is identified as responsive to Alk signaling. **c.** TaDa Pol II occupancy of *CG4577/Spar* shows decreased occupancy in Alk^{DN} experimental conditions compared to control. **d.** Expression of *CG4577/Spar* in w^{1118} (control), $Alk^{\Delta RA}$ (*Alk* loss-of-function allele) and Alk^{Y1355S} (*Alk* gain-of-function allele) larval CNS. Boxplot with normalized counts, **p<0.01, ***p<0.001. **e.** Feature plot showing mRNA expression of *CG4577/Spar* and *Alk* in third instar larval CNS scRNA-seq data. Neuroendocrine cluster is highlighted (red circle). **f.** CG4577/Spar-PA amino acid sequence indicating the signal peptide (amino acids 1-26, in red), glutamine repeats (in green) and the anti-CG4577/Spar antibody epitopes (amino acids 211-225 and 430-445, underlined). Center lines in boxplots indicate medians; box limits indicate the 25th and 75th percentiles; crosses represent sample means; whiskers extend to the maximum or minimum.
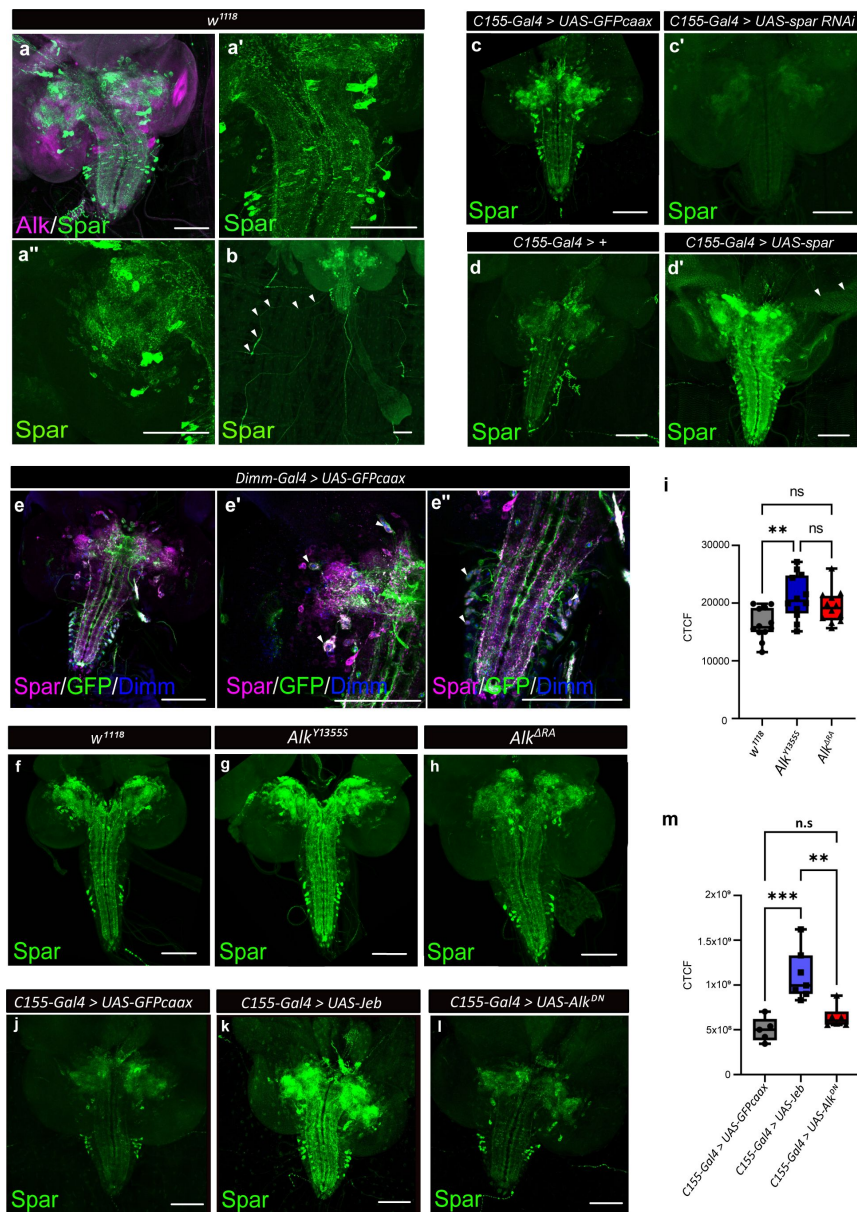
Figure 4.

Spar expression in the *Drosophila* larval brain.

a. Immunostaining of w^{1118} third instar larval brains with Spar (green) and Alk (magenta) revealing overlapping expression in central brain and ventral nerve cord. **a'-a''.** Close-up of Spar expression (green) in ventral nerve cord (a') and central brain (a''). **b.** Immunostaining of w^{1118} third instar larval CNS together with the body wall muscles, showing Spar (green) expression in neuronal processes (white arrowheads) which emerge from the ventral nerve cord and innervate larval body wall muscle number 8. **c-c'.** Decreased expression of Spar in third instar larval brains expressing *spar* RNAi (*C155-Gal4>Spar RNAi*) compared to control (*C155-Gal4>UAS-GFPcaax*) confirms Spar antibody specificity (Spar in green). **d-d'.** Spar overexpression (*C155-Gal4>UAS-Spar*) showing increased Spar expression (in green) compared to control (*C155-Gal4>+*) larval CNS. **e-e''.** Immunostaining of *Dimm-Gal4>UAS-GFPcaax* third instar larval brains with Spar (in magenta), GFP and Dimm (in blue) confirms Spar expression in Dimm-positive neuroendocrine cells (white arrowheads). **f-i.** Spar protein expression in w^{1118}, Alk^{Y1355S}, and $Alk^{\Delta RA}$ third instar larval brains. Quantification of Spar levels (corrected total cell fluorescence, CTCF) in **i.** **j-m.** Overexpression of Jeb in the third instar CNS (*C155-Gal4>UAS-Jeb*) leads to increased Spar protein expression compared to controls (*C155-Gal4>UAS-GFPcaax*). Quantification of Spar levels (corrected total cell fluorescence, CTCF) in **m.** (*******p*<0.01; ***p<0.001) Scale bars: 100 μm. Center lines in boxplots indicate medians; box limits indicate the 25th and 75th percentiles; whiskers extend to the maximum or minimum.

Spar expression is modulated in response to Alk signaling activity

Our initial integrated analysis predicted *Spar* as a locus responsive to Alk signaling. To test this hypothesis, we examined Spar protein expression in w^{1118}, Alk^{Y1355S} and $Alk^{\Delta RA}$ genetic backgrounds, in which Alk signaling output is either upregulated (Alk^{Y1355S}) or downregulated ($Alk^{\Delta RA}$) (Pfeifer *et al.,* 2022 ⧉). We observed a significant increase in Spar protein in Alk^{Y1355S} CNS, while levels of Spar in $Alk^{\Delta RA}$ CNS were not significantly altered (**Figure 4f-h** ⧉, quantified in **I**). In agreement, overexpression of Jeb *(C155-Gal4>jeb)* significantly increased Spar levels when compared with controls *(C155-Gal4>UAS-GFPcaax)* (**Figure 4j-l** ⧉, quantified in **m**). Again, overexpression of dominant-negative Alk *(C155-Gal4>UAS-Alk^{DN})* did not result in significantly decreased Spar levels (**Figure 4l** ⧉, quantified in **m**). Thus activation of Alk signaling increases Spar protein levels. However, while our bulk RNA-seq and TaDa datasets show a reduction in *Spar* transcript levels in Alk loss-of-function conditions, this reduction is not reflected at the protein level. This observation may reflect additional uncharacterized pathways that regulate *Spar* mRNA levels as well as translation and protein stability, since and notably *Spar* transcript levels are decreased but not absent in $Alk^{\Delta RA}$ (**Figure 3d** ⧉). Taken together, these observations confirm that *Spar* expression is responsive to Alk signaling in CNS, although Alk is not critically required to maintain Spar protein levels.

Spar encodes a canonically processed neurosecretory protein

To provide biochemical evidence for the expression of Spar, we re-analysed data from a previous LC-MS peptidomic analysis of brain extracts from five day old male control flies and flies deficient for carboxypeptidase D (dCPD, SILVER) (Pauls *et al*, 2019 ⧉), an enzyme that removes the basic C-terminal aa of peptides originating from proprotein convertases (PCs) cleavage of the proprotein. This analysis identified several peptides derived from the Spar propeptide by mass matching in non-digested extracts from genetic control brains (**Figure 5** ⧉). These included peptides that are framed by dibasic prohormone cleavage sequences in the propeptide, one of which (SEEASAVPTAD) was also obtained by *de-novo* sequencing (**Figure 5** ⧉). This result demonstrates that the Spar precursor is expressed and is processed into multiple peptides by PCs and possibly also other proteases. Analysis of the brain of *svr* mutant flies yielded similar results, but further revealed peptides C-terminally extended by the dibasic cleavage sequence (SEEASAVPTADKK, FNDMRLKR) (**Figure 5** ⧉), thereby confirming canonical PC processing of the Spar propeptide. Of note, the phylogenetically most conserved peptide sequence of the Spar precursor (DTQLNPADMLALVALVEAGERA, **Figure 3-figure supplement 2**) framed by dibasic cleavage sites was among the identified peptides yet occurred only in control but not *svr* mutant brains (**Figure 5** ⧉).

Additionally, we performed co-labeling with known *Drosophila* neuropeptides, Pigment-dispersing factor (PDF), Dh44, Insulin-like peptide 2 (Ilp2), AstA and Lk, observing Spar expression in subsets of all these populations (**Figure 6** ⧉). These included the PDF-positive LNv clock neurons (**Figure 6a-b** ⧉''), Dh44-positive neurons (**Figure 6c-d** ⧉''), a subset of Ilp2 neurons in the central brain (**Figure 6e-f** ⧉'') and several AstA-positive neurons in the central brain and ventral nerve cord (**Figure 6g-h** ⧉''). We also noted co-expression in some Lk-positive neurons in the central brain and ventral nerve cord, that include the neuronal processes converging on body wall muscle 8 (**Figure 6i-l** ⧉'') (Cantera & Nässel, 1992 ⧉). Similar Spar co-expression with PDF, Dh44, Ilp2, and AstA was observed in adult CNS (**Figure 6 – figure supplement 1**).

CRISPR/Cas9 generated *Spar* mutants are viable

Since previous reports have shown that Jeb overexpression in the larval CNS results in a small pupal size (Gouzi *et al.,* 2011 ⧉), we measured pupal size on ectopic expression of Spar (*C155-Gal4>Spar*) and Spar RNAi (*C155-Gal4>Spar RNAi*), noting no significant difference compared to controls (*C155-Gal4>+* and *C155-Gal4>jeb*) (**Figure** 7 – **figure supplement 1**). These results suggest that Spar may be involved in an additional Alk-dependant function in the CNS. Further,
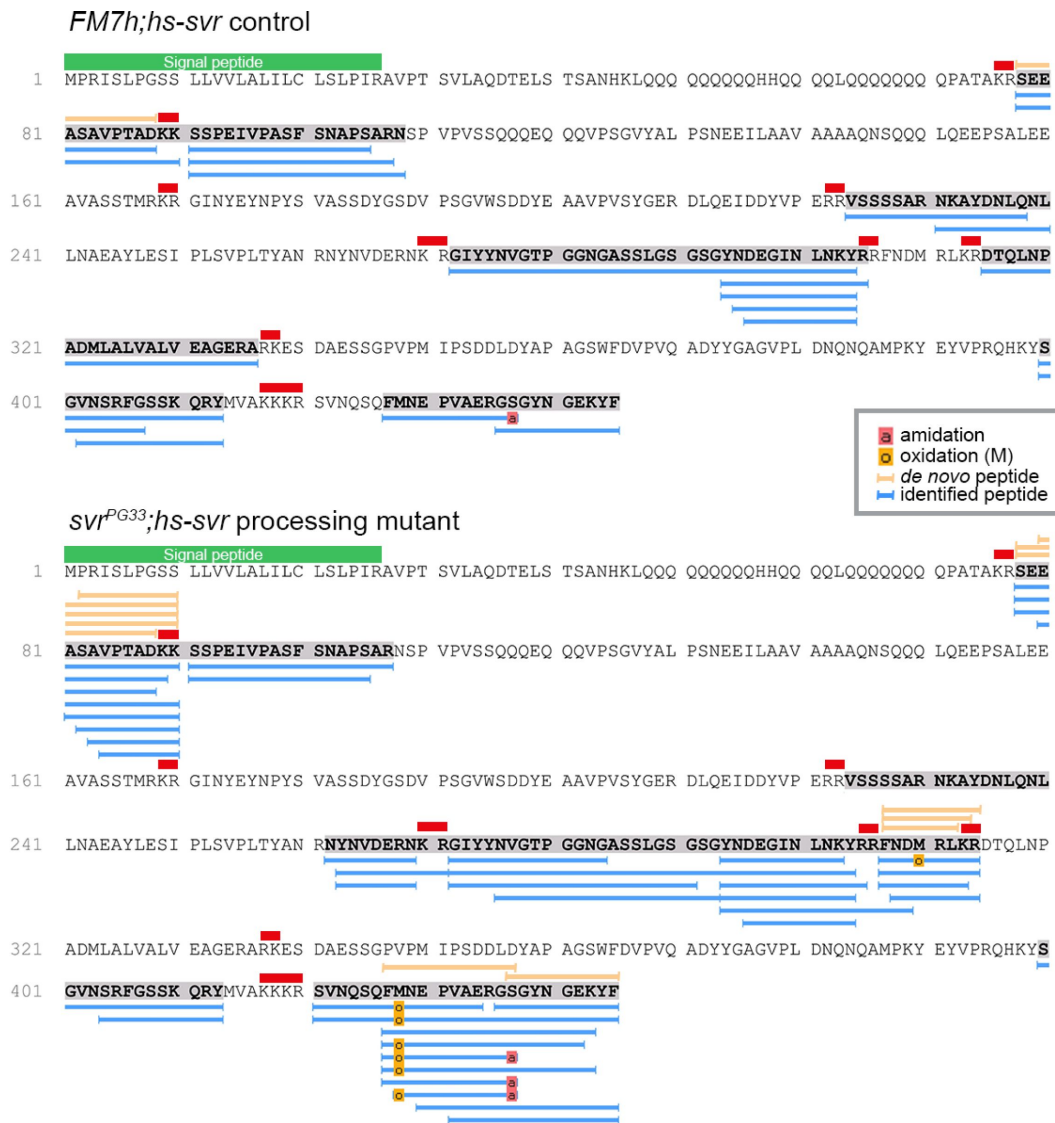
Figure 5.

Identification of Spar peptides in _Drosophila_ CNS tissues.

Peptides derived from the Spar prepropeptide identified by mass spectrometry in wild-type-like control flies (*FM7h;hs-svr*, upper panel) and *svr* mutant (*svrPG33;hs-svr*, lower panel) flies. The predicted amino acid sequence of the CG4577-PA Spar isoform is depicted for each genetic experimental background. Peptides identified by database searching (UniProt *Drosophila melanogaster*, 1% FDR) are marked by blue bars below the sequence. In addition, peptides correctly identified by *de novo* sequencing are marked by orange bars above the sequence. Red bars indicate basic prohormone convertase cleavage sites, green bar indicates the signal peptide.
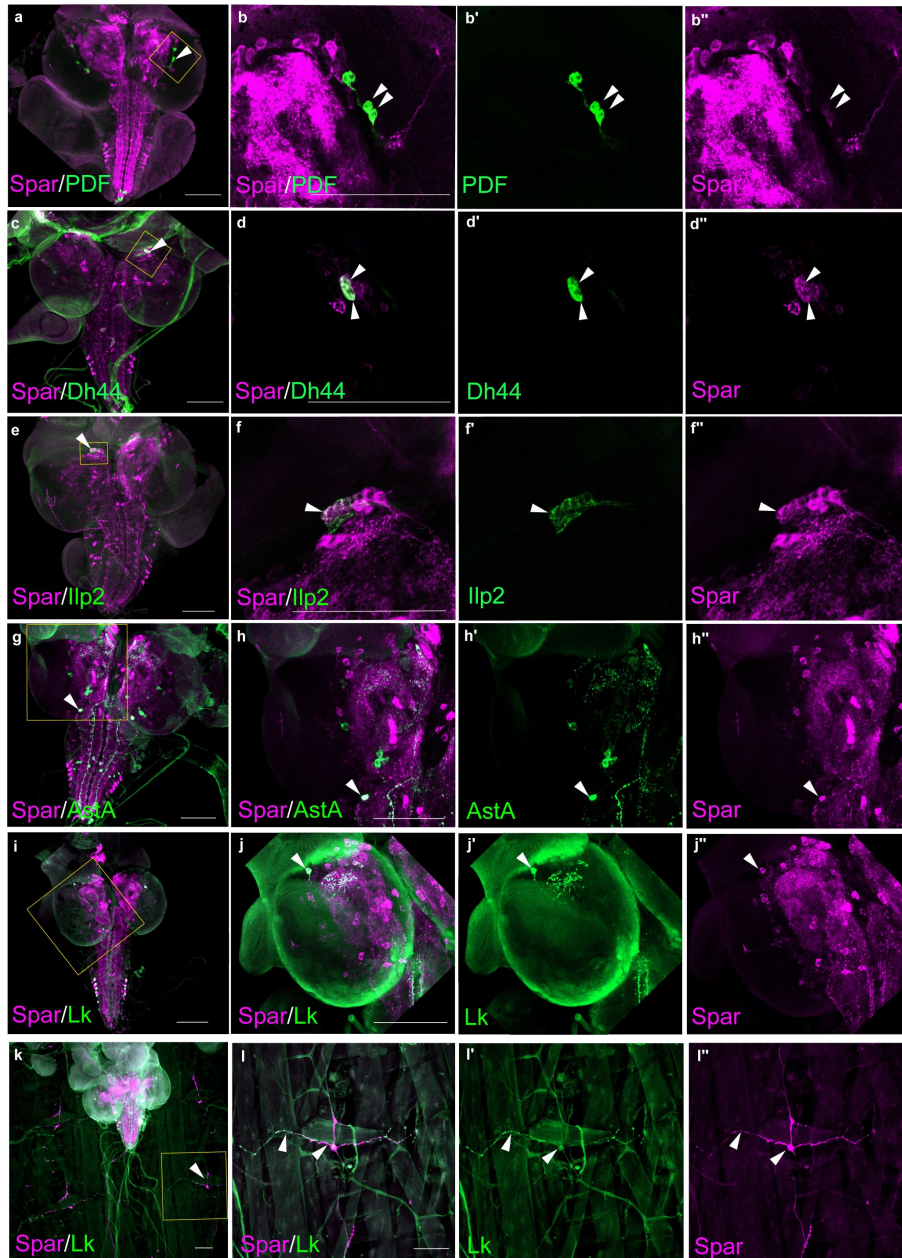
Figure 6.

***Spar* expression in larval neuropeptide expressing neuronal populations.**

a. Immunostaining of w^{1118} third instar larval CNS with Spar (in magenta) and PDF (in green). Closeups (**b-b''**) showing PDF- and Spar-positive neurons in central brain indicated by white arrowheads. **c.** Immunostaining of w^{1118} third instar larval CNS with Spar (in magenta) and Dh44 (in green). Closeups (**d-d''**) showing Dh44- and Spar-positive neurons in central brain indicated by white arrowheads. **e.** Immunostaining of w^{1118} third instar larval CNS with Spar (in magenta) and Ilp2 (in green). Closeups (**f-f''**) showing Ilp2- and Spar-positive neurons in central brain indicated by white arrowheads. **g.** Immunostaining of w^{1118} third instar larval CNS with Spar (in magenta) and AstA (in green). Closeups (**h-h''**) showing AstA- and Spar-positive neurons in central brain indicated by white arrowheads. **i.** Immunostaining of w^{1118} third instar larval CNS with Spar (in magenta) and Lk (in green). Closeups (**j-j''**) showing Lk (LHLK neurons)- and Spar-positive neurons in central brain indicated by white arrowheads. **k.** Immunostaining of w^{1118} third instar larval CNS together with the body wall muscles, showing Spar (in magenta) expressing Lk (in green) (ABLK neurons) in neuronal processes, which emerge from the ventral nerve cord and innervate the larval body wall muscle. Closeups (**l-l''**) showing co-expression of Lk and Spar in neurons which attach to the body wall number 8 indicated by white arrow heads. Scale bars: 100 μm.

experiments overexpressing Spar did not reveal any obvious phenotypes. To further investigate the function of Spar we generated a *Spar* loss of function allele by CRISPR/Cas9-mediated non-homologous end-joining, resulting in the deletion of a 716bp region including the *Spar* transcription start site and exon 1 (hereafter referred as *Spar^{ΔExon1}*) (**Figure 7a**). Immunoblotting analysis indicated a 35kDa protein present in the wild-type (w^{1118}) controls that was absent in *Spar^{ΔExon1}* mutant CNS lysates (**Figure 7b**). The *Spar^{ΔExon1}* mutant allele was further characterized using immunohistochemistry (**Figure 7c-d** '). *Spar^{ΔExon1}* shows a complete abrogation of larval and adult Spar expression, consistent with the reduction observed when *Spar* RNAi was employed (**Figure 7c-d** '). *Spar^{ΔExon1}* flies were viable, and no gross morphological phenotypes were observed, similar to loss of function mutants in several previously characterized neuropeptides such as Pigment-dispersing factor (PDF), Drosulfakinin (Dsk) and Neuropeptide F (NPF) (Liu *et al, 2019* ; Renn *et al, 1999* ; Wu *et al, 2020*).

Spar is expressed in a subset of clock-neurons in the larval and adult CNS

A previous report noted expression of *Spar* in the ventral lateral neuron (LNv), dorsal lateral neuron (LNd) and dorsal neuron 1 (DN1) populations of adult *Drosophila* circadian clock neurons (Abruzzi *et al, 2017*) (**Figure 7e** , **Table S1**). A meta-analysis of the publicly available single-cell transcriptomics of circadian clock neurons indicated that almost all adult cluster of clock neurons express *Spar* (Ma *et al, 2021*) (**Figure 7f**). Additionally, we noted that the expression of *Spar* peaks around Zeitgeber time 10 (ZT10) (coinciding with the evening peak of locomotor activity) (**Figure 7g-h**), although the differences in expression level around the clock with LD or DD cycle were not dramatic (**Figure 7 – figure supplement 2a-c**). To confirm the expression of Spar in circadian neurons at the protein level we co-stained Spar with a clock neuron reporter (*Clk856-Gal4>UAS-GFP*). A subset of Spar-positive larval CNS neurons appeared to be *Clk856-Gal4>UAS-GFP* positive (**Figure 7i-j** ''). Similarly, a subset of Spar-positive neurons in adults were GFP-positive (**Figure 7k-l** ''), confirming the expression of Spar protein in LNv clock neurons. Taken together, these findings suggest a potential function of the Alk-regulated TaDa-identified target Spar in the maintenance of circadian activity in *Drosophila*.

Spar^{ΔExon1} mutants exhibit reduced adult lifespan, activity and circadian disturbances

Given the expression of Spar in circadian neurons of the larval CNS, and the previous observations of a role of Alk mutations in sleep dysregulation in flies (Bai & Sehgal, 2015), we hypothesised that *Spar^{ΔExon1}* mutants may exhibit activity/circadian rhythm-related phenotypes. To test this, we first investigated the effects of loss of *Spar* (employing *Spar^{ΔExon1}*) and loss of *Alk* (employing a CNS specific loss of function allele of *Alk*, *Alk^{ΔRA}* (Pfeifer *et al*., 2022)) on adult lifespan and sleep/activity behaviour using the DAM (*Drosophila* activity monitor) system (Trikinetics Inc.). Both *Alk^{ΔRA}* and *Spar^{ΔExon1}* mutant flies displayed a significantly reduced lifespan when compared to w^{1118} controls, with the *Spar^{ΔExon1}* group exhibiting a significant reduction in survival at 25 days (**Figure 8a**). Activity analysis in *Alk^{ΔRA}* and *Spar^{ΔExon1}* flies under 12 h light: 12 h dark (LD) conditions indicated that both *Alk^{ΔRA}* and *Spar^{ΔExon1}* flies exhibited two major activity peaks, the first centered around Zeitgeber time 0 (ZT0), the beginning of the light phase, the so-called morning peak, and the second around Zeitgeber time 12 (ZT12), the beginning of the dark phase that is called the evening peak (**Figure 8b** , **black arrows**). Overall activity and sleep profiles per 24 h showed increased activity in *Spar^{ΔExon1}* flies (**Figure 8b-d** , **Figure 8 – figure supplement 1**), that was more prominent during the light phase, with an increase in the anticipatory activity preceding both the night-day and the day-night transition in comparison to *Alk^{ΔRA}* and w^{1118} (**Figure 8b** , **empty arrows**). Actogram analysis over 30 days showed an increased number of activity peaks in the mutant groups, indicating a hyperactivity phenotype, in comparison to wild-type (**Figure 8d**). Furthermore, mean activity and sleep were also affected;
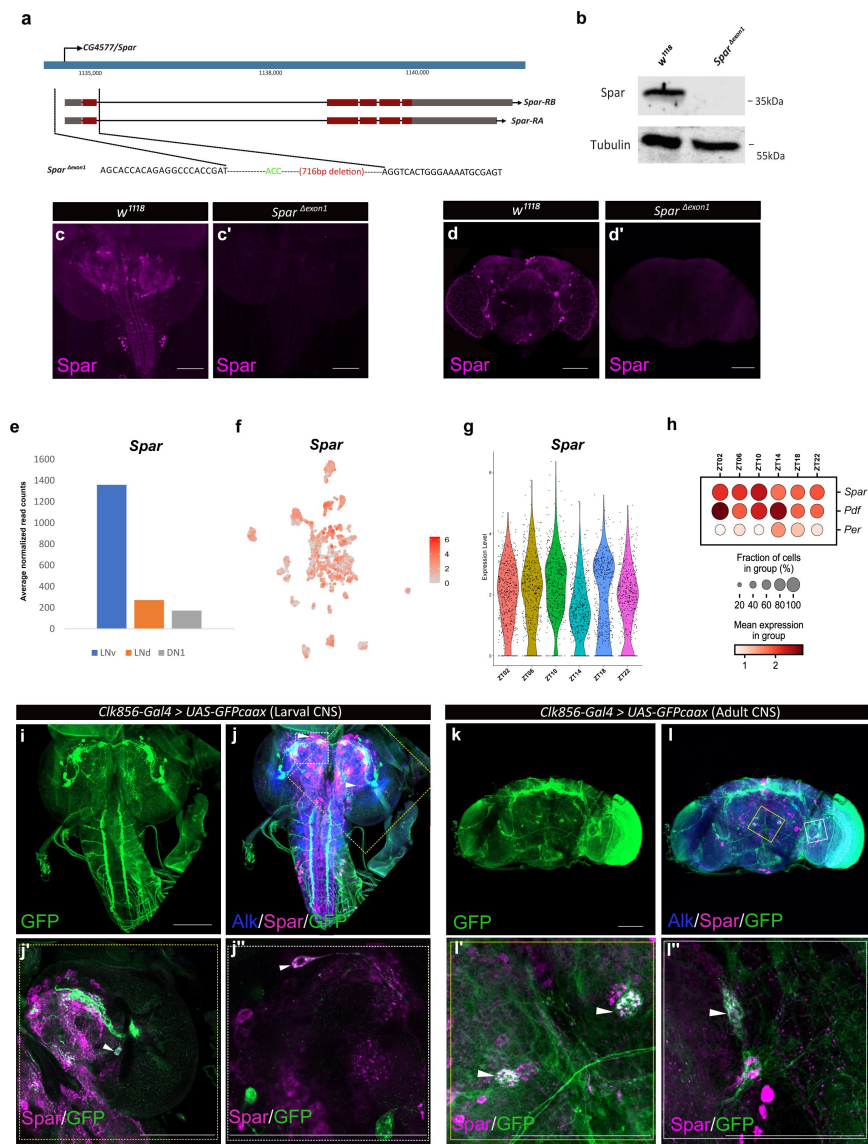
Figure 7.

Generation of $Spar^{\Delta Exon1}$ mutant and expression of *Spar* in circadian neurons.

a. Schematic overview of the *Spar* gene locus and the $Spar^{\Delta Exon1}$ mutant. Black dotted lines indicate the deleted region, which includes the transcriptional start and exon 1. **b.** Immunoblotting for Spar. Spar protein (35 kDa) is present in larval CNS lysates from wild-type (w^{1118}) controls but absent in $Spar^{\Delta Exon1}$ mutants. **c-d'.** Immunostaining confirms loss of Spar protein expression in the $Spar^{\Delta Exon1}$ mutant. Third instar larval **(c-c')** and adult **(d-d')** CNS stained for Spar (in magneta). Spar signal is undetectable in $Spar^{\Delta Exon1}$. **e.** Expression of *Spar* in LNv, LNd and DN1 circadian neuronal populations, employing publicly available RNA-seq data (Abruzzi *et al*., 2017). **f.** Feature plot of *Spar* expression in circadian neurons, employing publicly available scRNA-seq data (Ma *et al*., 2021). **g.** Violin plot indicating *Spar* expression throughout the LD cycle, showing light phase (ZT02, ZT06 and ZT10) and dark phase (ZT14, ZT18 and ZT22) expression. **h.** Dotplot comparing *Spar* expression throughout the LD cycle with the previously characterized circadian-associated neuropeptide pigment dispersion factor (*Pdf*) and the core clock gene Period *(per)*. Expression levels and percentage of expressing cells are indicated. **i-j.** Spar expression in clock neurons (*Clk856-Gal4>UAS-GFPcaax*) of the larval CNS **(i-j)**, visualized by immunostaining for Spar (magenta), Alk (in blue) and clock neurons (GFP, in green). **j'-j''.** Close up of central brain regions (yellow dashed box in **j**) indicating expression of Spar in Clk856-positive neurons (white arrowheads). **k-l.** Immunostaining of *Clk856-Gal4>UAS-GFPcaax* in adult CNS with GFP (in green), Spar (in magenta) and Alk (in blue). **l'-l''.** Close ups of CNS regions (yellow dashed box in **l**) stained with GFP (in green) and Spar (in red) showing a subset of clock-positive neurons expressing Spar (white arrowheads). Scale bars: 100 μm.

the two mutant groups ($Alk^{\Delta RA}$ and $Spar^{\Delta Exon1}$) displayed significant variations in activity means (**Figure 8e** ☑ **, h-h'; Figure 8 – figure supplement 2**). To further consolidate these results, we evaluated the anticipatory activity by quantifying activity in the 6 h period before lights-on (a.m. anticipation) or lights-off (p.m. anticipation) as previously described {Harrisingh, 2007 #5159}; $Spar^{\Delta Exon1}$ flies exhibited a significant increase in this anticipatory activity both in the night-day and day-night transition (**Figure 8f-g** ☑). Furthermore, both $Alk^{\Delta RA}$ and $Spar^{\Delta Exon1}$ exhibited significant decrease in average sleep during the day per 12 h at young ages (days 5 to 7) (**Figure 8h** ☑ **, Figure 8 – figure supplement 2a**). In contrast, older flies (days 20 to 22) did not show any significant differences in sleep patterns during the day and per 12 h (**Figure 8h** ☑ **', Figure 8 – figure supplement 2a'**). The decrease in average sleep in both Alk$^{\Delta RA}$ and $Spar^{\Delta Exon1}$ was accompanied by an increase in number of sleep bouts per 12 hours at young age (days 5 to 7) (**Figure 8 – figure supplement 2b**) with no difference in number of sleep bouts at older age (**Figure 8 – figure supplement 2b'**). Rhythmicity analysis showed that $Alk^{\Delta RA}$ and w^{1118} are more rhythmic in LD compared to $Spar^{\Delta Exon1}$ flies **(Figure 8 – figure supplement 3a)**, however when comparing percentage of rhythmic flies among all groups the differences were not significant **(Figure 8 – figure supplement 3a')**. Moreover, free-running period calculation by Chi-square periodograms showed that both w^{1118} and $Spar^{\Delta Exon1}$ flies exhibit a longer circadian period (higher than 1440 minutes), with 13% of the latter group having a shorter period **(Figure 8 – figure supplement 4a-a')**. These results demonstrate that Spar is important for normal fly activity and loss of spar affects adult sleep/wake activity.

Since $Spar^{\Delta Exon1}$ flies exhibited a hyperactive phenotype during both day and night hours, we sought to investigate a potential role of *Spar* in regulating the endogenous fly clock by assessing fly activity after shift to dark conditions. While control flies adapted to the light-dark shift without any effect on mean activity and sleep, $Spar^{\Delta Exon1}$ flies exhibited striking defects in circadian clock regulation (**Figure 9a-b** ☑ **', Figure 8 – figure supplement 1a-d'**). Comparison of average activity and sleep during 5 days of LD (light-dark) versus 5 days of DD (dark-dark) cycles, identified a reduction in mean activity under DD conditions in $Spar^{\Delta Exon1}$ flies (**Figure 9b-b** ☑ **').** Actogram profiling showed that $Spar^{\Delta Exon1}$ flies exhibit a hyperactive profile consistent with our previous data in LD conditions and maintain this hyperactivity when shifted into DD conditions (**Figure 9c** ☑ **, Figure 8 – figure supplement 1**). Further, anticipatory peaks were largely absent on transition to DD cycle in $Spar^{\Delta Exon1}$ mutants with no activity peaks observed at either CT0 or at CT12 (**Figure 9b** ☑ **, empty arrows**), consistent with a significant decrease in the a.m and p.m anticipatory activity (**Figure 8g** ☑ **)** and altered activity and sleep bouts in these mutants (**Figure 9d** ☑ **, Figure 8** ☑ **– figure supplement 2**). To confirm that the circadian clock activity defects observed here were specific to loss of *Spar* we conducted a targeted knockdown of *Spar* in clock neurons, employing *Clk856-Gal4. Clk856-Gal4>Spar-RNAi* flies exhibited a significant disruption in both activity and sleep during the DD transition period, consistent with a hyperactivity phenotype (**Figure 9e-f** ☑ **', Figure 9 – figure supplement 1**). Further comparison of *Clk856-Gal4>Spar-RNAi* flies relative to control identified a consistent increase in activity in both LD and DD conditions upon *Spar* knockdown, with a decrease in sleep observed in DD conditions (**Figure 9 – figure supplement 2**). These findings agree with the expression pattern of *Spar* in clock neurons (**Figure 7** ☑), indicating a role for Spar in circadian clock regulation. Rhythmicity analysis comparing LD and DD cycles in $Spar^{\Delta Exon1}$ did not show a significant change indicating that $Spar^{\Delta exon1}$ flies are mostly rhythmic in LD and DD conditions, whereas as expected, control w^{1118} flies were less rhythmic in DD conditions (**Figure 9 – figure supplement 3a-a'**). This was also consistent when percentages of rhythmicity were determined, both w^{1118} and $Spar^{\Delta exon1}$ flies were rhythmic **(Figure 9 – figure supplement 3b-b')**. In terms of circadian period, the majority of w^{1118} and $Spar^{\Delta exon1}$ flies exhibited a longer free running period both in LD and DD (**Figure 9 – figure supplement 3c-d**).
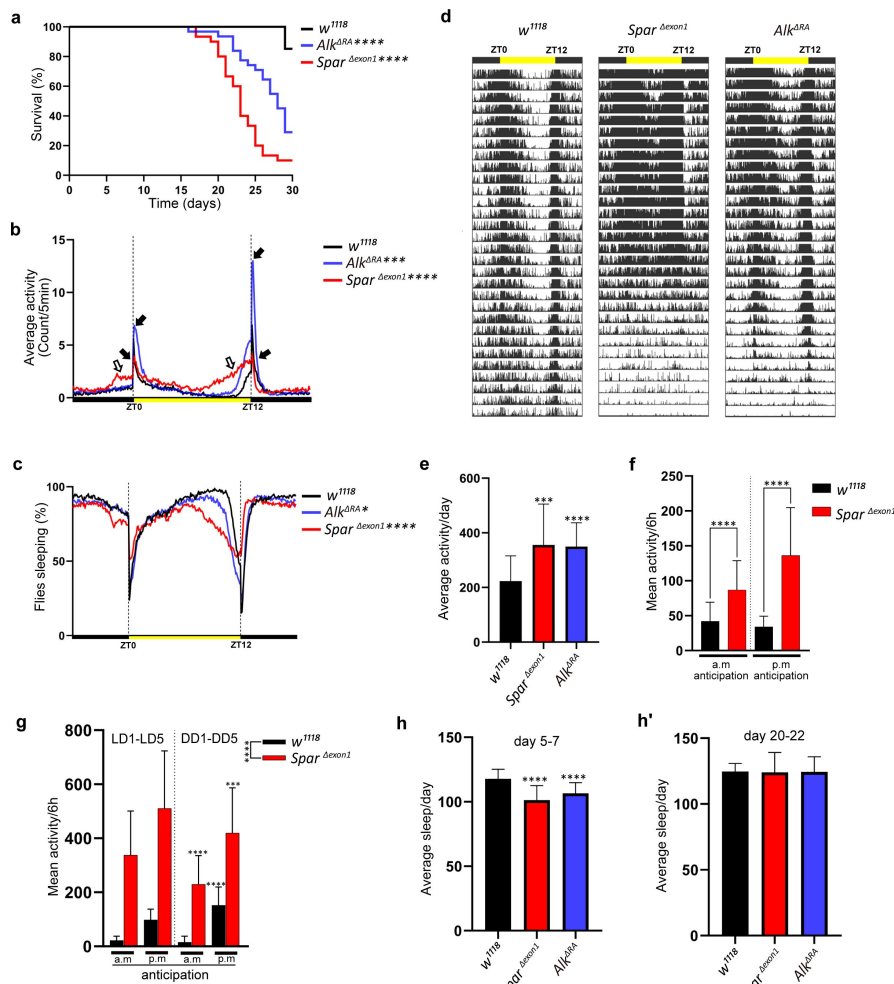
Figure 8.

Lifespan and activity plots of *Spar^{ΔExon1}* mutants.

a. Kaplan-Meier survival curve comparing *Alk^{ΔRA}* (n=31) and *Spar^{ΔExon1}* (n=30) flies to *w^{1118}* controls (n=27). Outliers from each group were determined by Tukey's test, and statistic al significance was analyzed by Log-rank Mantel-Cox test (****p<0.0001). **b.** Representative activity profile graph illustrating average activity count measured every 5 min across a 24 h span. Black arrows indicate morning and evening activity peaks. Empty arrows indicate anticipatory increase in locomotor activity of *Spar^{ΔExon1}* mutant flies occurring before light transition. Unpaired student t-test was used to determine significance between control and mutant groups (****p<0.0001; ***p<0.001). **c.** Representative sleep profile graph illustrating the percentage of time that flies spend sleeping measured every 5 min across a 24 h span. Unpaired student t-test was used to determine significance between control and mutant groups (****p<0.0001; *p<0.05). **d.** Representative average actogram of individual flies in each group. Each row corresponds to one day, visualized as 288 bars each representing one 5 min interval. Yellow bar represents the time of the day when the lights are turned on, with ZT0 indicating the morning peak and ZT12 the evening peak. **e.** Mean locomotor activity per day across a 30-day span. Unpaired student t-test was used to determine significance between control and mutant groups (****p<0.0001; ***p<0.001). **f.** Mean locomotor activity for 6 h intervals over 14 days. a.m. anticipation and p.m. anticipation depict mean activity in the 6 h before lights on and 6 h before lights off respectively. Unpaired student t-test was used to determine the significance between control and *Spar^{ΔExon1}* (****p<0.0001). **g.** Mean locomotor activity for 6 h intervals over 5 days in LD and 5 days in DD conditions. The a.m. and p.m. anticipation depict mean activity in the 6 h before lights on (or subjective lights on) and 6 h before lights off (or subjective lights off) respectively. Unpaired student t-test was used to determine the significance between *Spar^{ΔExon1}* and controls (****p<0.0001); paired student t-test was used to determine significance in each group between the two experimental conditions (****p<0.0001; ***p<0.001). Mean sleep per day across a 3-day average (Day 5-7 (h), Day 20-22 (h')). Unpaired student t-test was used to determine significance between control and mutant groups (****p<0.0001). The error bars in the bar graphs represents standard deviation.
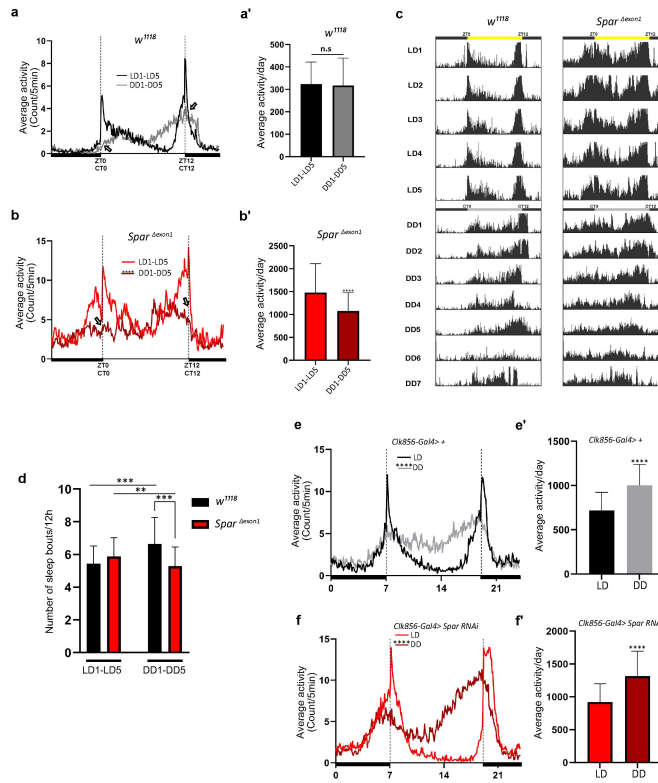
Figure 9.

$Spar^{\Delta Exon1}$ mutants exhibit circadian activity disturbances

a. Representative activity profile for w^{1118} controls, illustrating the average activity count measured every 5 min across a 24 h span for Light-Dark (LD) for 5 cycles (black line), subsequently switching to Dark-Dark (DD) for 5 cycles (gray lines). ZT0 and ZT12 represent the start and end of the photoperiod respectively. CT0 and CT12 represent the start and end of the subjective day in constant dark conditions. Empty arrows indicate morning and evening peaks at CT0 and CT12 respectively. Paired student t-test was used to determine significance. **a'.** Mean locomotor activity per day in controls obtained by averaging 5 days in light/dark conditions (LD1-LD5) and 5 days in dark/dark conditions (DD1-DD5). Paired student t-test was used to determine significance. **b.** Representative activity profile graph of $Spar^{\Delta Exon1}$ illustrating the average activity count measured every 5 min across 24 h obtained by averaging 5 days in light/dark conditions (LD1-LD5) and 5 days in dark/dark conditions (DD1-DD5). Empty arrows indicate morning and evening peaks at CT0 and CT12 respectively. Paired student t-test was used to determine significance between the two experimental conditions (****p<0.0001). **b'.** Mean locomotor activity per day of $Spar^{\Delta Exon1}$ obtained by averaging 5 days in light/dark conditions (LD1-LD5) and 5 days in dark/dark conditions (DD1-DD5). Paired student t-test was used to determine significance (****p<0.0001). **c.** Representative average actograms of individual w^{1118} flies (n=32) and $Spar^{\Delta Exon1}$ flies (n=31) in LD and DD conditions. Each row corresponds to one day, visualized in 288 bars each representing one 5 min interval. ZT0 and ZT12 represent the start and end of the photoperiod respectively. CT0 and CT12 represent the start and end of the subjective day in constant dark conditions. **d.** Average number of sleep bouts for 12 h lights on intervals over 5 days in LD and 5 days in DD conditions. Unpaired student t-test was used to determine significance between control (w^{1118}) and $Spar^{\Delta Exon1}$ (***p<0.001). Paired student t-test was used to determine significance between the two experimental conditions (***p<0.001; **p<0.01). **e.** Representative activity profile graph of $Clk856-Gal4$>+ illustrating the average activity count measured every 5 min across a 24 h span for Light-Dark (LD) for 5 cycles (black line) and subsequently switching to Dark-Dark (DD) for 5 cycles (gray lines). Paired student t-test was used to determine significance (****p<0.0001). **e'.** Mean locomotor activity per day of $Clk856-Gal4$>+ obtained by averaging 5 days in light/dark conditions (LD1-LD5) and 5 days in dark/dark conditions (DD1-DD5). Paired student t-test was used to determine significance (****p<0.0001). **f.** Representative activity profile graph of $Clk856-Gal4$>$UAS-Spar$ $RNAi$ illustrating the average activity count measured every 5 min across 24 h span obtained by averaging 5 days in light/dark conditions (LD1-LD5) and 5 days in dark/dark conditions (DD1-DD5). Paired student t-test was used to determine significance (****p<0.0001). **f'.** Mean locomotor activity per day for $Clk856-Gal4$>$UAS-Spar$ $RNAi$ obtained by averaging 5 days in light/dark conditions (LD1-LD5) and 5 days in dark/dark conditions (DD1-DD5). Paired student t-test was used to determine the significance (****p<0.0001). Error bars represent standard deviation.

Discussion

With the advent of multiple omics approaches, data integration represents a powerful, yet challenging approach to identify novel components and targets of signaling pathways. The availability of various genetic tools for manipulating Alk signaling in *Drosophila* along with previously gathered omics dataset provides an excellent basis for Alk centered data acquisition. We complemented this with TaDa transcriptional profiling allowing us to generate a rich dataset of Alk-responsive loci with the potential to improve our mechanistic understanding of Alk signaling in the CNS. A striking observation revealed by integrating our TaDa study with scRNAseq data was the enrichment of Alk-responsive genes expressed in neuroendocrine cells. These results are consistent with previous studies reporting expression of Alk in the *Drosophila* larval prothoracic gland (Pan & O'Connor, 2021), the neuroendocrine functions of Alk in mice (Ahmed *et al.*, 2022 ; Reshetnyak *et al*, 2015 ; Witek *et al.*, 2015) and the role of oncogenic ALK in neuroblastoma, a childhood cancer which arises from the neuroendocrine system (Matthay *et al.*, 2016 ; Umapathy *et al.*, 2019). In this study, we focused on one target of interest downstream of Alk, however, many additional interesting candidates remain to be explored. These include *CG12594*, *complexin* (*cpx*) and the *vesicular glutamate transporter* (*VGlut*) that also exhibit a high ratio of co-expression with *Alk* in scRNAseq data **(Supplementary** Figure 1**)**. A potential drawback of our TaDa dataset is the identification of false positives, due to non-specific methylation of GATC sites at accessible regions in the genome by Dam protein. Hence, our experimental approach likely more reliably identifies candidates which are downregulated upon Alk inhibition. In our analysis, we have limited this drawback by focusing on genes downregulated upon Alk inhibition and integrating our analysis with additional datasets, followed by experimental validation. This approach is supported by the identification of numerous previously identified Alk targets in our TaDa candidate list.

Employing a strict context dependent filter on our integrated omics datasets identified Spar as a previously uncharacterized Alk regulated neuropeptide precursor. Spar amino acid sequence analysis predicts an N-terminal signal peptide and multiple canonical dibasic PC cleavage sites which are hallmarks of neuropeptide precursors. This is strong indication that Spar is shuttled to the secretory pathway and is post-translationally processed within the Golgi or transport vesicles. Moreover, using mass spectrometry, we were able to identify predicted canonically processed peptides from the Spar precursor in undigested fly brain extracts. While all this points towards a neuropeptide-like function of Spar, other features appear rather unusual for a typical insect neuropeptide. First, the Spar propeptide is quite large for a neuropeptide precursor, and the predicted peptides do not represent paracopies of each other and do not carry a C-terminal amidation signal as is typical for *Drosophila* and other insect peptides (Nässel & Zandawala, 2019 ; Wegener & Gorbashov, 2008). Moreover, there are no obvious Spar or Spar peptide orthologues in animals outside the Diptera. We noted, however, that Spar is an acidic protein with a pI of 5.1 that lacks any cysteine residue. These features are reminiscent of vertebrate secretogranins, which are packaged and cleaved by PCs and other proteases inside dense vesicles in the regulated secretory pathway in neurosecretory cells (Helle, 2004). Secretogranins have so far not been identified in the *Drosophila* genome (Hart *et al*, 2017). Therefore, the identification of the neurosecretory protein Spar downstream of Alk in the *Drosophila* CNS is particularly interesting in light of previous findings, where VGF (aka secretogranin VII) has been identified as one of the strongest transcriptional targets regulated by ALK in both cell lines and mouse neuroblastoma models (Borenas *et al.*, 2021 ; Cazes *et al*, 2014). *VGF* encodes a precursor polypeptide, which is processed by PCs generating an array of secreted peptide products with multiple functions that are not yet fully understood at this time (Lewis *et al*, 2015 ; Quinn *et al*, 2021).

Using a newly generated antibody we characterized the expression of Spar in the *Drosophila* CNS, showing that its expression overlaps with the Dimm transcription factor that is expressed in the fly neuroendocrine system (Hewes *et al.*, 2003), suggesting that Spar is expressed along with

multiple other neuropeptides in pro-secretory cells of the CNS (Park *et al.*, 2008). Spar is also expressed in well-established structures such as the mushroom bodies (Crocker *et al*, 2016) (Table 1), which are known to be important in learning and memory and regulate food attraction and sleep (Joiner *et al*, 2006 ; Pitman *et al*, 2006), and where Alk is also known to function (Bai & Sehgal, 2015 ; Gouzi *et al.*, 2011 ; Pfeifer *et al.*, 2022). Interestingly, Spar is expressed in a subset of peptidergic neurons which emerge from the ventral nerve cord (VNC) and innervate larval body wall muscle number 8. In larvae, these Lk-expressing neurons of the VNC, known as ABLKs, are part of the circuitry that regulates locomotion and nociception, and in adults they regulate water and ion homeostasis (Imambocus *et al*, 2022 ; Okusawa *et al*, 2014 ; Zandawala *et al*, 2018). The role of Spar in this context is unknown and requires further investigation. The identity of the Spar receptor, as well as its location, both within the CNS and without, as suggested by the expression of Spar in neurons innervating the larval body wall is another interesting question for a future study. In our current study we focused on characterising Spar in the *Drosophila* CNS. To functionally characterize Spar in this context we generated null alleles with CRISPR/Cas9 and investigated the resulting viable $Spar^{\Delta Exon1}$ mutant.

Spar transcript expression in *Drosophila* clock neurons has been noted in a previous study investigating neuropeptides in clock neurons, however Spar had not been functionally characterized at the time (Abruzzi *et al.*, 2017 , Ma *et al*, 2021). We have been able to show that Spar protein is expressed in clock neurons of the larval and adult CNS, findings that prompted us to study the effect of Spar in activity and circadian rhythms of flies. *Drosophila* activity monitoring experiments with $Spar^{\Delta Exon1}$ and Alk loss of function ($Alk^{\Delta RA}$) mutants revealed striking phenotypes in life span, activity and sleep. In *Drosophila* a number of genes and neural circuits involved in the regulation of sleep have been identified (Shafer & Keene, 2021). The role of Alk in sleep has previously been described in the fly, where Alk and the Ras GTPase Neurofibromin1 (Nf1), function together to regulate sleep (Bai and Sehgal, 2015). Indeed, a study in mice has reported an evolutionarily conserved role for Alk and Nf1 in circadian function (Weiss *et al*, 2017). While these studies place Alk and Nf1 together in a signaling pathway that regulates sleep and circadian rhythms, no downstream effectors transcriptionally regulated by the Alk pathway have been identified that could explain its regulation of *Drosophila* sleep/activity. Our data suggest that one way in which Alk signaling regulates sleep is through the control of Spar, as $Spar^{\Delta Exon1}$ mutants exhibit a striking activity phenotype. The role of clock neurons and the involvement of circadian input in maintenance of long term memory (LTM) involving neuropeptides such as PDF has been previously described (Inami *et al*, 2022). Since both Alk and Nf1 are also implicated in LTM formation in mushroom body neurons (Gouzi, Bouraimi et al 2018), the potential role of Nf1 in Spar regulation and the effect of Spar loss on LTM will be interesting to test in future work. It can be noted that insulin producing cells (IPCs), DH44 cells of the pars intercerebralis, the Lk producing LHLK neurons of the brain and certain AstA neurons in the brain are involved in regulation of aspects of metabolism and sleep (Barber *et al*, 2021 ; Cavey *et al*, 2016 ; Chen *et al*, 2016 ; Cong *et al*, 2015 ; Donlea *et al*, 2018 ; Nässel & Zandawala, 2022 ; Yurgel *et al*, 2019). Furthermore, the DH44 cells of the pars intercerebralis are major players in regulation feeding and courtship in adults (Barber *et al.*, 2021 ; Cavanaugh *et al*, 2014 ; Dus *et al*, 2015 ; King *et al*, 2017 ; Oh *et al*, 2021).

In conclusion, our TaDa analysis identifies a role for Alk in regulation of endocrine function in *Drosophila*. These results agree with the previously reported broad role of Alk in functions such as sleep, metabolism, and olfaction in the fly and in the hypothalamic-pituitary-gonadal axis and Alk-driven neuroblastoma responses in mice. Finally, we identify *Spar* as the first neuropeptide precursor downstream of Alk to be described that regulates activity and circadian function in the fly.

Materials and methods

Drosophila stocks and Genetics

Standard *Drosophila* husbandry procedures were followed. Flies were fed on Nutri-Fly® Bloomington Formulation food (Genesee Scientific, Inc.) cooked according to the manufacturer's instruction. Crosses were reared at 25°C. The following stocks were obtained from Bloomington *Drosophila* Stock Center (BDSC): w^{1118} (BL3605), *Dimm-Gal4* (also known as *C929-Gal4*) (BL25373), *Clk856-Gal4* (BL93198) and *C155-Gal4* (BL458). The *UAS-Spar RNAi* (v37830) line was obtained from Vienna Drosophila Resource Center. Additional stocks used in this study are the following: *UAS-LT3-NDam-Pol II* (Southall *et al*., 2013), *UAS-Alk^{DN}* (P{UAS-Alk.EC.MYC} (Bazigou *et al*., 2007)), *UAS-Jeb* (Varshney & Palmer, 2006), *UAS-GFPcaax* {Finley, 1998 #2378}, *Alk^{Y1335S}* (Pfeifer *et al*., 2022), *Alk$^{\Delta RA}$* (Pfeifer *et al*., 2022), *Spar$^{\Delta Exon1}$* (this study), *UAS-Spar* (this study).

TaDa Sample preparation

Pan neuronal *C155-Gal4* expressing animals were crossed with either *UAS-LT3-Dam::Pol II* (Control) or *UAS-LT3-Dam::Pol II; UAS-Alk^{EC}* (Alk dominant negativ e sample) and crosses were reared at 25°C. Approximately 100-150 third instar larval brains were dissected in cold PBS for each technical replicate. Genomic DNA was extracted using a QIAGEN blood and tissue DNA extraction kit and methylated DNA was processed and amplified as previously described (Choksi *et al*, 2006 ; Sun *et al*, 2003) with the following modifications; after genomic DNA extraction, non-sheared gDNA was verified on 1.5% agarose gel, and an overnight DpnI digestion reaction set up in a 50 µl reaction volume. The digestion product was subsequently purified using QIAGEN MiniElute PCR purified Kit and eluted in 50 µl MQ water. 50 µl of DpnI digested and purified DNA was further used for adaptor ligation. Adaptor ligated DNA was amplified using the adaptor specific primer to generate the TaDa-seq library. Amplified DNA from all experimental conditions was repurified (QIAGEN MiniElute PCR purification kit) into 20 µl of MQ water and 200 ng aliquots were run on 1% agarose gel to verify amplification of TaDa library (DNA fragments ranging from 500 bp to 3 kb). The TaDa library was used for PCR-free library preparation followed by paired-end sequencing on an Illumina HiSeq 10x platform (BGI Tech Solutions, Hong Kong).

TaDa bioinformatics data analysis

TaDa FASTQ paired-end reads of the control sample with three biological replicates and dominant negative samples with two biological replicates (with two technical replicates for both control and dominant negative samples) were obtained for a total of 10 samples and used for subsequent analysis. After base quality assessment, reads were mapped to the Dm6 reference genome of *Drosophila melanogaster* using Bowtie2 (--very-sensitive-local) (Langmead & Salzberg, 2012) and post alignment processes were performed with sam tools and BED tools (Barnett *et al*, 2011 ; Quinlan, 2014). The *Drosophila melanogaster* reference sequence (FASTA) and gene annotation files were downloaded from Flybase and all GATC coordinates were extracted using fuzznuc (Rice *et al*, 2000) in BED format. Replicates were merged using Sambamba (merge) (Tarasov *et al*, 2015), and fold changes between control and dominant negative samples, obtained by deeptools bamCompare (--centerReads --scaleFactorsMethod readCount --effectiveGenomeSize 142573017 -- smoothLength 5 -bs 1) (Ramirez *et al*, 2014) for BIGWIG (BW) file generation. Counts of reads mapped to GATC border fragments were generated using a perl script (GATC_mapper.pl) from DamID-Seq pipeline (Maksimov *et al*, 2016). GATC level counts were converted to gene level counts using Bedtools (intersectBed) (Quinlan, 2014). GATC sites were merged into peaks based on a previous study (Tosti et al., 2018). Log2FC for individual GATC sites were generated using Limma for dominant negative vs control (P < 1e-5) and GATC sites were merged into peaks based on median GATC fragment size in the *Drosophila* genome assembly using mergeWindows (tol=195, max.width=5000) and combineTests function from the csaw package (Lun & Smyth, 2016). Peaks were assigned to overlapping genes and filtered for FDR smaller than 0.05 and mean log2FC less than -2. All peak calling and statistical analysis was performed using the R programming

environment. TaDa data can also be visualized using a custom UCSC (University of California, Santa Cruz) Genome Browser session (*https://genome-euro.ucsc.edu/s/vimalajeno/dm6*). WebGestaltR (Liao *et al*, 2019) was used for GO (Gene Ontology) for significantly downregulated TaDa candidates.

Integration of TaDa data with scRNA-seq and other omics data

Previously published wild-type third instar larval brain scRNA-Seq data (GSE198850) was employed (Pfeifer *et al.*, 2022). Cellular heterogeneity was determined with eight different types of cells, including immature neurons, mature neurons, early neuroblast, NB-enriched cells, NB proliferating cells, optic lobe epithelium (OLE), Repo-positiv e cells and Wrapper-positive cells. The mature neuron population was divided into two groups for the current study: mature neurons and neuroendocrine cells. The neuroendocrine cell cluster was determined based on canonical markers (Guo *et al.*, 2019 ; Huckesfeld *et al.*, 2021 ; Nässel, 2018 ; Takeda & Suzuki, 2022 ; Torii, 2009). Subsequent analysis, including dimensionality reduction/projection or cluster visualization and marker identification was performed using R (Seurat) (Stuart *et al*, 2019) and Python (Scanpy) (Wolf *et al*, 2018) packages. Marker genes for each cluster were identified by FindAllMarkers function (Seurat) (Stuart *et al.*, 2019). Clusters were visualized using two-dimensional Uniform Manifold Approximation and Projection (UMAP). The top 500 significantly downregulated genes from TaDa data (FDR<0.05 and mean logFC≤-2) were analysed in the third instar larval brain scRNAseq data. These 500 candidates were used as gene signatures, and signature enrichment analysis carried out using AUCell to determine whether a subset of the input gene set was enriched for each cell (with an enrichment threshold set at >0.196), and the clusters projected in UMAP based on the signature score (AUC score) (Aibar *et al.*, 2017). Violin plots, dot plots, feature plots, heatmaps and matrix plots were used to visualize gene expression in the scRNAseq data. Functional enrichment analysis for the common significantly downregulated genes from the TaDa analysis was compared to neuroendocrine cell markers using WebGestaltR (Liao *et al.*, 2019).

Circadian neuron scRNA-Seq data analysis

Publicly available circadian neuron scRNA-Seq data (10x) from the GEO database (GSE157504) was employed to investigate expression of *CG4577* in circadian neurons (Ma *et al.*, 2021). The dataset includes two conditions: LD (Light and Dark) and DD (Dark and Dark), as well as six time points: 2 hours, 6 hours, 10 hours, 14 hours, and 22 hours. After preprocessing, 3172 and 4269 cells remained for the LD and DD samples respectively, with a total of 15,743 and 15,461 RNA features. Subsequent analysis, including integration, dimensionality reduction/projection and cluster visualization was performed using R (Seurat) (Stuart *et al.*, 2019). Based on clustering, 17 clusters were defined and visualized using two-dimensional Uniform Manifold Approximation and Projection (UMAP). Violin plots, dot plots, and feature plots were employed to visualize gene expression.

Immunohistochemistry

Relevant tissue (larval CNS or body wall muscle preparation) was dissected in cold PBS and tissues fixed in 4% formaldehyde at 4°C for 1 hour. Samples were washed 3 times with 0.1% PBS Triton X-100, followed by overnight incubation in 4% goat serum, 0.1% PBS Triton X-100. The following primary antibodies were used: guinea pig anti-Alk (1:1000, (Loren *et al.*, 2003)), rabbit anti-Alk (1:1000, (Loren *et al.*, 2003)), and rabbit anti-Dimm (1:1000 (Allan *et al*, 2005)), chicken anti-GFP (1:1000, Abcam #ab13970), mouse mAb anti-PDF (1:1000, DSHB: C7), rabbit anti-Ilp2 (1:1000, (Veenstra *et al*, 2008)), anti-Dh44 (1:1000, (Cabrero *et al*, 2002)), rabbit anti-AstA (1:3000, (Stay *et al*, 1992) (Vitzthum *et al*, 1996), Jena Bioscience GmbH), rabbit anti-Lk (1:1000, (Cantera & Nässel, 1992)), guinea pig anti-Spar (1:2000, this study), and Alexa Fluor®-conjugated secondary antibodies were from Jackson Immuno Research.

Image Analysis

Spar fluorescence intensity (**Figures 4I** ⧉ and M) was quantified for the minimum complete confocal z-series of each third instar larval brain using Fiji (Schindelin et al, 2012). Confocal images from the 488 nm wavelength channel were analyzed as a Z project. Using a selection tool, Spar positive areas were demarcated, and measurements recorded. Corrected total cell fluorescence (CTCF), in arbitrary units, was measured for each third instar brain as follows: CTCF = integrated density – (area of selected cell × mean fluorescence of background readings) (McCloy RA, et al. Cell Cycle. 2014; Bora P, et al. Commun Biol 2021). Calculated CTCFs were represented in the form of boxplots (n = 12 each for w^{1118}, Alk^{Y1255S}, Alk^{RA}. n = 5 each for *C155-Gal4>UAS-GFPcaax* and *C155-Gal4>UAS-Alk^{DN}*, n = 7 for *C155-Gal4>UAS-Jeb*).

Immunoblotting

Third instar larval brains were dissected and lysed in cell lysis buffer (50 mM Tris-Cl, pH7.4, 250 mM NaCl, 1 mM EDTA, 1 mM EGTA, 0.5% Triton X-100, complete protease inhibitor cocktail and PhosSTOP phosphatase inhibitor cocktail) on ice for 20 minutes prior to clarification by centrifugation at 14,000 rpm at 4°C for 15 minutes. Protein samples were then subjected to SDS-PAGE and immunoblotting analysis. Primary antibodies used were: guinea pig anti-Spar (1:1000) (this study) and anti-tubulin (Cell Signaling #2125, 1:20,000). Secondary Antibodies used were: Peroxidase Affinipure Donkey Anti-Guinea Pig IgG (Jackson ImmunoResearch #706-035-148) and goat anti-rabbit IgG (Thermo Fisher Scientific # 32260, 1:5000).

Generation of anti-Spar antibodies

Polyclonal antibodies against Spar (CG4577) were custom generated in guinea pigs by Eurogentec. Two Spar peptides corresponding to epitopes LQEIDDYVPERRVSS (amino acids 212-226) and PVAERGSGYNGEKYF (amino acids 432-446) of Spar-PA were injected simultaneously.

Biochemical identification of Spar peptides and phylogenetic analysis

Peptidomic data from our previous study on the role of *Drosophila* carboxypeptidase D (SILVER) in neuropeptide processing (Pauls *et al.,* 2019 ⧉) was re-examined for the occurrence of Spar. Peptides were extracted from brains from 5 d old male flies and analyzed on an Orbitrap Fusion mass spectrometer (Thermo Scientific) equipped with a PicoView ion source (New Objective) and coupled to an EASY-nLC 1000 system (Thermo Scientific). Three (controls) and two (mutants) biological samples (pooled brain extracts from 30 flies) were measured in technical duplicates. The raw data is freely available at Dryad (*https://doi.org/10.5061/dryad.82pr5td* ⧉, for details see (Pauls *et al.,* 2019 ⧉)). Database search was performed against the UniProt Drosophila melanogaster database (UP000000803; 22070 protein entries) with PEAKS XPro 10.6 software (Bioinformatics solution) with the following parameters: peptide mass tolerance: 8 ppm, MS/MS mass tolerance: 0.02 Da, enzyme: "none"; variable modifications: Oxidation (M), Carbamidomethylation (C), Pyro-glu from Q, Amidation (peptide C-term). Results were filtered to 1% PSM-FDR.

To identify Spar precursor sequences in other insects and arthropods, tblastn searches with the PAM30 matrix and a low expectation threshold against the whole *Drosophila* Spar precursor or partial peptides flanked by canonical cleavage sites were performed against the NCBI databank (*https://blast.ncbi.nlm.nih.gov/Blast.cgi* ⧉). The obtained sequences were aligned by the MUSCLE algorithm and plotted using JalView 2{Waterhouse, 2009 #5160}.

CRISPR/Cas9 mediated generation of the *Spar^{ΔExon1}* mutant

The *Spar^{ΔExon1}* mutant was generated using CRISPR/Cas9 genome editing. Design and evaluation of CRISPR target sites was performed using the flyCRISPR Optimal Target Finder tool (Gratz et al., 2015). Single guide RNA (sgRNA) targeting sequences (sequences available in **Table S1**) were

cloned into the pU6-BbsI-chiRNA vector (Addgene, Cat. No. 45946) and injected into *vasa-Cas9* (BDSC, #51323) embryos (BestGene Inc.). Injected flies were crossed to second chromosome balancer flies (BDSC, #9120) and their progeny were PCR-screened for a deletion event. Mutant candidates were confirmed by Sanger sequencing (Eurofins Genomics).

Generation of *UAS-Spar* fly lines

UAS-Spar was generated by cloning (GeneScript) the coding sequence of *CG4577-RA* into EcoRI/XbaI-cut *pUASTattB* vector followed by injection into fly embryos (BestGene Inc.) using attP1 (2nd chromosome, BDSC#8621) and attP2 (3rd chromosome, BDSC#8622) docking sites for phiC31 integrase-mediated transformation. Injected flies were crossed to second or third chromosome balancer flies, and transgenic progeny identified based on the presence of mini-white marker.

Measurement of pupal size

Late pupae of the indicated genotype were collected and placed on glass slides with double-sided tape. Puparium were imaged with a Zeiss Axio Zoom.V16 stereo zoom microscope with a light-emitting diode ring light and measured using Zen Blue edition software. Both female and male pupae, picked randomly, were used for measurements.

Drosophila activity monitor assay

Up to 32 newly eclosed male flies were transferred into individual glass tubes containing food media (1% agar and 5% sucrose), which were each placed into a DAM2 *Drosophila* activity monitor (Trikinetics Inc). Monitors were then placed in a 25°C incubator running a 12:12h light:dark cycle, at a constant 60% humidity. Activity was detected by an infrared light beam emitted by the monitor across the center of each glass tube. The experiment was carried out for one month, and the raw binary data was acquired by the DAMSystem310 software (Trikinetics Inc.). The LD/DD experiment was performed according to previously published work (Chiu *et al*, 2010); adult flies were first entrained for 5 days in normal light:dark cycle and on the last day (LD5), the light parameters were switched off and flies were then conditioned in complete dark:dark settings for 7 days. Statistical and data analyses were carried out using Microsoft Office and GraphPad Prism 8.4.2, taking into consideration 5 min of inactivity as sleep and more than 24 h of immobility as a death event. Actogram activity profile charts were generated using ActogramJ 1.0 (*https://bene51 .github.io/ActogramJ/index.html*) and ImageJ software (*https://imagej.nih.gov/ij/*). ActogramJ was further used to generate the chi-square periodogram for each single fly in order to calculate the power value of rhythmicity and the percentage of rhythmic flies.

Data visualization and schematics

Schematics were generated at *Biorender.com* and Bioicons.com. The pipeline icon by Simon Dürr *https://twitter.com/simonduerr* is licensed under CC0 *https://creativecommons.org/publicdomain /zero/1.0/* . Boxplots in **Figure 3d** and **Figure 7** – figure supplement 1 were generated using BoxplotR (*http://shiny.chemgrid.org/boxplotr/*). Boxplots in **Figure 4** were generated using GraphPad Prism 9.

Datasets used in this study

Dataset name	Brief description	Reference	NCBI gene Expression omnibus ID/database IDs
Targeted DamID (TaDa) dataset	Pol II occupancy of control (*UAS-Dam-Pol II*) and *Alk* knockdown (*UAS-Dam-Pol II*; *Alk^{DN}*) conditions in 3rd instar *Drosophila* larval CNS.	This study	GSE229518
Bulk RNA-seq dataset - *Drosophila Alk* allels	Transcripomes of Alk gain-of-function (*Alk^{Y1355S}*), Alk CNS specific loss-of-function (*Alk^{RA}*) and control (*w^{1118}*) 3rd instar *Drosophila* larval CNS.	Pfeifer *et al.*, 2022	GSE198812
3rd instar Larval CNS Single cell RNA-seq dataset	Single cell transcriptome of control (*w^{1118}*) *Drosophila* 3rd instar larval CNS.	Pfeifer *et al*, 2022	GSE198850
1st instar larval CNS Single cell RNA-seq dataset	Single cell transcriptome of control (*Canton-S*) *Drosophila* 1st instar larval CNS.	Brunet Avalos *et al.*, 2019	GSE134722
Adult CNS single cell RNA-seq dataset	Single cell transcriptome of control (*w^{1118}*) *Drosophila* adult brains.	Davie *et al.*, 2018	GSE107451
Adult CNS peptidomics data	Peptidomic mass spectrometry analysis of control (*FM7h;hs-svr*) and SILVER processing mutant (*svr^{PG33};hs-svr*) in *Drosophila* adult brains.	Pauls *et al.*, 2019	Dryad: https://doi.org/10.5061/dryad.82pr5td
Bulk RNA-seq dataset - *Drosophila* circadian clock neurons	Transcriptome of circadian clock neurons from *Drosophila* adult brains.	Abruzzi *et al.*, 2017	GSE77451
Single cell RNA-seq dataset - Drosophila circadian clock neurons	Single cell transcriptome of circadian clock neurons (*Clk856-Gal4>EGFP*) in *Drosophila* adult brains.	Ma et al, 2021	GSE157504

Acknowledgements

Author contributions

SKS and RHP conceived the research. Wet lab experiments were conducted by SKS, LM, JS, MK, GU, PM-G, and TM. VA carried out all bioinformatics analysis. LM assisted with *Spar* mutant generation, validation, and immunohistochemistry. JS and MK performed and analyzed all *Drosophila* activity monitoring experiments under the supervision of MS. GU performed immunoblotting. PM-G assisted in optimizing and performing TaDa experiments, and TM performed image analysis and assisted with immunohistochemistry. AS and CW analyzed mass spectrometry peptidomic data and performed the phylogenetic analysis. DN provided critical feedback and design input. RHP, CW and MS supervised the project. SKS and RHP wrote the first manuscript draft that was further developed with all authors.

Competing interests

The authors declare that they have no competing interests

Data Availability Statement

Supplementary figure legends

Figure 1 – figure supplement 1. TaDa third instar larval CNS sample validation and additional data analysis. a-b'. Expression of mCherry in the larval CNS reflects Dam-PolII expression. Third instar larval brains were stained for Alk (in green) and mCherry (in red) confirming expression of Dam-PolII in the TaDa system. Scale bars: 100 µm. **c.** Schematic overview of the TaDa analysis experimental workflow. Brains from third instar wandering larvae were dissected, and methylated DNA digested with Dpn1 restriction endonuclease. The resulting DNA fragment library was amplified, sequenced and analysed through TaDa bioinformatics pipelines. **d.** Bar graph showing total number of reads in each replicate of the TaDa dataset. **d'.** Bar graph showing percentage of reads aligned to *Drosophila* genome in each replicate. **e.** Correlation plot of samples (*control* and *Alk^{DN}*) and replicates shows no significant intra-replicate differences. **f.** Line graph indicating the relative distance to TSS of different samples compared to random regions. **g.** Pol ll occupancy profile of *Alk* in *Alk^{DN}* compared to control indicates a higher pol II occupancy in exons 1 to exon 7, in agreement with the expression of the *Alk^{DN}* transgene.

Figure 2 – figure supplement 1. a-a''. Alk staining in *Dimm-Gal4>UAS-GFPcaax* third instar larval CNS confirms Alk expression in Dimm-positive cells. Alk (in magenta) and GFP (in green), close-ups indicating overlapping cells (indicated by yellow arrowheads) in the larval ring gland corpora cardiaca cells **(b-b'')** central brain **(c-c'')** and ventral nerve cord **(d-d'')**. Scale bars: 100 µm.

Figure 3 – figure supplement 1. Co-expression of *Alk* and *Spar* in publicly available *Drosophila* CNS scRNA-seq datasets. UMAP showing co-expression of *Alk* and *CG4577* in different cell clusters in publicly available scRNA-seq datasets (Brunet Avalos *et al.*, 2019 ⤢) from first instar larval CNS **(a)** and **(b)** adult CNS (Davie *et al.*, 2018 ⤢). **c.** Pairwise alignment of CG4577-PA and CG4577-PB showing isoform-specific differences at amino acid positions 405 and 406 (highlighted in yellow).

Figure 3 – figure supplement 2. Alignment of *CG4577* orthologs in flies (Brachycera). a. Alignment of *Drosophila melanogaster CG4577* orthologs in the family *Drosophilidae* (vinegar flies, including the fruit fly *Drosophila melanogaster)*. **b.** Alignment of *Drosophila melanogaster CG4577* orthologs in other brachyceran taxa.

Figure 4 – figure supplement 1. a-a'' Immunostaining of *w^{1118}* third instar larval brains with Spar (green) and Alk (magenta) revealing overlapping expression (indicated by yellow arrowheads) in central brain, ring gland corpora cardiaca and ventral nerve cord. Close-ups indicating overlapping cells in central brain **(b-b''**, corresponding to dashed box on left in A**)** and ring gland corpora cardiaca cells **(c-c''**, corresponding to dashed box on right in A**)**. Scale bars: 100 µm.

Figure 4 – movie supplement 1. Z-stack projection video of **Figure 4e** ⤢'

Figure 4 – movie supplement 2. Z-stack projection video of **Figure 4e** ⤢''

Figure 4 – figure supplement 2. a-a'' Adult CNS showing Spar expression in Dimm-positive cells. Spar (in magenta) and Dimm (in green), close-ups **(b-b'')** indicated by boxed region and white arrows indicating representative co-expressed markers cells. Scale bars: 100 μm.

Figure 6 – figure supplement 1. *Spar* **expression in adult neuropeptide expressing neuronal populations**. **a.** Immunostaining of w^{1118} adult CNS with anti-Spar (in magenta) and anti-PDF (in green). Closeups **(b-b'')** of PDF- and Spar-positiv e LNv neurons, indicated by white arrowheads. **c.** Immunostaining of w^{1118} adult CNS with Spar (in magenta) and Dh44 (in green). Closeups **(d-d'')** of Dh44- and Spar-positive neurons, indicated by white arrowheads. **e.** Immunostaining of w^{1118} adult CNS with Spar (in magenta) and Ilp2 (in green). Closeups **(f-f'')** showing the close proximity and overlap of Ilp2-positive and Spar-positive neurons in central brain, indicated by white arrowheads. **g.** Immunostaining of w^{1118} adult CNS with Spar (in magenta) and AstA (in green). Closeups **(h-h'')** showing AstA- and Spar-positiv e neurons in central brain indicated by white arrowheads. Scale bars: 100μm.

Figure 7 – figure supplement 1. Spar does not affect the Alk-regulated pupal size phenotype. Overexpression of Spar (*C155-Gal4>UAS-Spar*) or *Spar RNAi* (*C155-Gal4>UAS-Spar RNAi*) in CNS does not significantly affect pupal size compared to previously characterized controls such as Alk^{DN} (*C155-Gal4>UAS-Alk^{DN}*), which significantly increases pupal size and overexpression of *Jeb* (*C155-Gal4>UAS-Alk^{DN}*), which significantly decreases pupal size compared to controls (*C155-Gal4>+*) (n.s = not significant, **p<0.05, ***p<0.01). Center lines in boxplots indicate medians; box limits indicate the 25th and 75th percentiles; whiskers extend 1.5 times the interquartile range from the 25th and 75th percentiles, crosses represent sample means; grey bars indicate 83% confidence intervals of the means; data points are plotted as grey circles.

Figure 7 – figure supplement 2. *Spar* **expression in circadian neuronal clusters. a-b.** Feature plots depicting the expression of *Spar* in publicly available circadian neuronal scRNA-seq data (Ma *et al.,* 2021 ☑) throughout the LD cycle (Zeitgeber time) **(a)** and DD cycle (Circadian time) **(b). c.** Dotplot showing *Spar* expression throughout the DD cycle along with the previously characterized circadian associated neuropeptide *Pdf* and the core clock gene *Per*. Peak expression of *Spar* and *Per* is observed at CT10.

Figure 8 – figure supplement 1. a. Representative activity profile graph of control (w^{1118}) and $Spar^{\Delta Exon1}$ illustrating average activity count measured every 5 min across a 24 h span obtained by averaging 5 days in light/dark conditions (LD1-LD5). Unpaired student t-test was used to determine significance (****p<0.0001). **a'.** Mean locomotor activity per day of control and $Spar^{\Delta Exon1}$ obtained by averaging 5 days in light/dark conditions (LD1-LD5). Unpaired student t-test was used to determine significance (****p<0.0001). **b.** Representative activity profile graph of control and $Spar^{\Delta Exon1}$ illustrating the average activity count measured every 5 min across a 24 h span obtained by averaging 5 days in dark/dark conditions (DD1-DD5). CT0 and CT12 represent the start and end of the subjective day in constant dark conditions respectively. Unpaired student t-test was used to determine significance (****p<0.0001). **b'.** Mean locomotor activity per day for control and $Spar^{\Delta Exon1}$ obtained by averaging 5 days in dark/dark conditions (DD1-DD5). Unpaired student t-test was used to determine significance (****p<0.0001). **c.** Representative sleep profile graph of control and $Spar^{\Delta Exon1}$ illustrating the average activity count measured every 5 min across a 24 h span obtained by averaging 5 days in light/dark conditions (LD1-LD5). Unpaired student t-test was used to determine significance (****p<0.0001). **c'.** Graph illustrating mean sleep per day of control and $Spar^{\Delta Exon1}$ obtained by averaging 5 days in light/dark conditions (LD1-LD5). Unpaired student t-test was used to determine significance (****p<0.0001). **d.** Representative sleep profiles of controls and $Spar^{\Delta Exon1}$ illustrating the average activity count measured every 5 min across a 24 h span obtained by averaging 5 days in dark/dark conditions (DD1-DD5). Unpaired student t-test was used to determine significance (****p<0.0001). **d'.** Mean sleep per day of control and $Spar^{\Delta Exon1}$ obtained by averaging 5 days in dark/dark conditions (DD1-DD5). Unpaired student t-test was used to determine significance (****p<0.0001). Error bars represent standard deviation.

Figure 8 – figure supplement 2. a-a'. Mean sleep per 12 h lights on intervals over 3 days (Day 5-7 (**a**), Day 20-22 (**a'**)). Unpaired student t-test was used to determine significance between control and mutant groups (****$p<0.0001$). **b-b'.** Graph illustrating the average number of sleep bouts for 12 h lights on intervals over 3 days (Day 5-7 (**b**), Day 20-22 (**b'**)). Unpaired student t-test was used to determine the significance between controls and mutant groups (****$p<0.0001$). Error bars represent standard deviation.

Figure 8 – figure supplement 3. $Spar^{\Delta Exon1}$ flies retain a hyperactive profile when shifted to dark/dark conditions. a. Graph illustrating the Qp statistical value (rhythmicity power) obtained by generating Chi-square periodograms of control (w^{1118}), $Spar^{\Delta Exon1}$, and $Alk^{\Delta RA}$ flies. Unpaired student t-test was used to determine significance between controls and each mutant group (****$p<0.0001$). **a'.** Representative graph of percentage of rhythmicity of w^{1118}, $Spar^{\Delta Exon1}$, and $Alk^{\Delta RA}$ flies. Error bars represent standard deviation.

Figure 8 – figure supplement 4. a. Graph illustrating the percentage of arrhythmic flies, and flies with a free-running period higher or lower than 1440 minutes (24 h). Flies were maintained under LD conditions and 14 days were selected to calculate the free-running period by generating Chi-Square periodograms for each fly in the group. Only data from rhythmic flies was selected to calculate the percentage of flies having a higher or lower period than 1440 minutes. **a'.** Average free-running periods of flies over 14 days in LD conditions. Flies with an arrhythmic profile were not selected for statistical analysis. Unpaired student t-test was used to determine significance between the two groups. Error bars represent standard deviation.

Figure 9 – figure supplement 1. a. Representative sleep profile graph of *Clk856-Gal4>+* illustrating the percentage of time sleeping measured every 5 min across a 24 h span obtained by averaging 5 days in light/dark conditions (LD1-LD5) and 5 days in dark/dark conditions (DD1-DD5). Paired student t-test was used to determine significance (****$p<0.0001$). **a'.** Mean sleep per day of *Clk856-Gal4>+* obtained by averaging 5 days in light/dark conditions (LD1-LD5) and 5 days in dark/dark conditions (DD1-DD5). Paired student t-test was used to determine significance (****$p<0.0001$). **b.** Representative sleep profile graph of *Clk856-GAL4>Spar RNAi* illustrating the percentage of time sleeping measured every 5 min across a 24 h span obtained by averaging 5 days in light/dark conditions (LD1-LD5) and 5 days in dark/dark conditions (DD1-DD5). Paired student t-test was used to determine significance (****$p<0.0001$). **b'.** Mean sleep per day of *Clk856-GAL4>Spar RNAi* obtained by averaging 5 days in light/dark conditions (LD1-LD5) and 5 days in dark/dark conditions (DD1-DD5). Paired student t-test was used to determine significance (****$p<0.0001$). Error bars represent standard deviation.

Figure 9 – figure supplement 2. a. Representative activity profile graph of control (w^{1118}) and *Clk856-Gal4>Spar RNAi* illustrating the average activity count measured every 5 min across a 24 h span obtained by averaging 5 days in light/dark conditions (LD1-LD5). Unpaired student t-test was used to determine significance (**$p<0.01$). **a'.** Mean locomotor activity per day of control and *Clk856-Gal4>Spar RNAi* obtained by averaging 5 days in light/dark conditions (LD1-LD5). Unpaired student t-test was used to determine significance (**$p<0.01$). **b.** Representativ e activity profile graph of control and *Clk856-Gal4>Spar RNAi* illustrating the average activity count measured every 5 min across a 24-hour span obtained by averaging 5 days in dark/dark conditions (DD1-DD5). Unpaired student t-test was used to determine significance (****$p<0.0001$). **b'.** Mean locomotor activity per day of control and *Clk856-Gal4>Spar RNAi* obtained by averaging 5 days in dark/dark conditions (DD1-DD5). Unpaired student t-test was used to determine the significance between the two groups (***$p<0.001$). **c.** Representative sleep profile graph of control and *Clk856-Gal4>Spar RNAi* illustrating the average activity count measured every 5 min across a 24 h span obtained by averaging 5 days in light/dark conditions (LD1-LD5). Unpaired student t-test was used to determine significance. **c'.** Mean sleep per day of control and *Clk856-Gal4>Spar RNAi* obtained by averaging 5 days in light/dark conditions (LD1-LD5). Unpaired student t-test was used to determine significance. **d.** Representative sleep profile graph of control and *Clk856-Gal4>Spar*

RNAi illustrating the average activity count measured every 5 min across a 24 h span obtained by averaging 5 days in dark/dark conditions (DD1-DD5). Unpaired student t-test was used to determine significance (*p<0.05). **d'.** Mean sleep per day of control and *Clk856-Gal4>Spar RNAi* obtained by averaging 5 days in dark/dark conditions (DD1-DD5). Unpaired student t-test was used to determine significance (**p<0.01). Error bars represent standard deviation.

Figure 9 – figure supplement 3. a. Qp statistical value obtained by generating Chi-square periodograms of control (w^{1118}) flies in 5 days LD and 7 days DD conditions. Paired student t-test was used to determine significance (***p<0.001). **a'.** Qp statistic al value obtained by generating Chi-square periodograms of $Spar^{\Delta Exon1}$ flies in 5 days LD and 7 days DD conditions. Paired student t-test was used to determine significance. **b.** Percentage rhythmicity of control (w^{1118}) flies in LD vs DD conditions. **b'.** Percentage rhythmicity of $Spar^{\Delta Exon1}$ flies in LD vs DD conditions. **c.** Percentage of flies with a free-running period higher or lower than 1440 minutes (24 h). Flies were maintained for 5 days under LD conditions and shifted to 7 days under DD. The free-running period was calculated by generating Chi-Square periodograms for each fly in the group. Only data from rhythmic flies was selected to calculate the percentage of flies having a period higher or lower than 1440 minutes. **d.** Graph illustrating the average free-running periods of flies over 5 days in LD and 7 days in DD conditions. Flies with an arrhythmic profile were not selected for the statistical analysis. An unpaired student t-test was used to determine the significance between the two groups (**p<0.01). Error bars represent standard deviation.

Additional Supplementary information

Supplementary Figure 1. Feature plots visualizing expression of TaDa-identified genes expressed in neuroendocrine cells in scRNA-seq from third instar larval CNS (Pfeifer *et al.,* 2022 ⧉). TaDa candidates *CG12594, cpx* and *VGlut* are shown.

Supplementary Table 1. TaDa data Alk^{DN} downregulated genes (Sheet 1). RNASeq normalized read count data of *CG4577* in control (w^{1118}), Alk^{RA} and Alk^{Y1355S} conditions (Sheet 2). RNAseq average normalized read count data of *Spar* in LNv, LNd and DN1 clock neuronal cells (Sheet 3). $Spar^{\Delta Exon1}$ mutant CRISPR single guide RNA target and screening primer information (Sheet 4).

References

Abruzzi KC, Zadina A, Luo W, Wiyanto E, Rahman R, Guo F, Shafer O, Rosbash M (2017) **RNA-seq analysis of Drosophila clock and non-clock neurons reveals neuron-specific cycling and novel candidate neuropeptides** *PLoS Genet* **13**

Ahmed M, Kaur N, Cheng Q, Shanabrough M, Tretiakov EO, Harkany T, Horvath TL, Schlessinger J (2022) **A hypothalamic pathway for Augmentor alpha-controlled body weight regulation** *Proc Natl Acad Sci U S A* **119**

Aibar S *et al.* (2017) **SCENIC: single-cell regulatory network inference and clustering** *Nat Methods* **14**:1083–1086

Allan DW, Park D, St Pierre SE, Taghert PH, Thor S (2005) **Regulators acting in combinatorial codes also act independently in single differentiating neurons** *Neuron* **45**:689–700

Almagro Armenteros JJ, Tsirigos KD, Sonderby CK, Petersen TN, Winther O, Brunak S, von Heijne G, Nielsen H (2019) **SignalP 5.0 improves signal peptide predictions using deep neural networks** *Nat Biotechnol* **37**:420–423

Bai L, Sehgal A (2015) **Anaplastic Lymphoma Kinase Acts in the Drosophila Mushroom Body to Negatively Regulate Sleep** *PLoS Genet* **11**

Barber AF, Fong SY, Kolesnik A, Fetchko M, Sehgal A (2021) **Drosophila clock cells use multiple mechanisms to transmit time-of-day signals in the brain** *Proc Natl Acad Sci U S A*

Barnett DW, Garrison EK, Quinlan AR, Stromberg MP, Marth GT (2011) **BamTools: a C++ API and toolkit for analyzing and managing BAM files** *Bioinformatics (Oxford, England)* **27**:1691–1692

Bazigou E, Apitz H, Johansson J, Loren CE, Hirst EM, Chen PL, Palmer RH, Salecker I (2007) **Anterograde Jelly belly and Alk receptor tyrosine kinase signaling mediates retinal axon targeting in Drosophila** *Cell* **128**:961–975

Bilsland JG *et al.* (2008) **Behavioral and neurochemical alterations in mice deficient in anaplastic lymphoma kinase suggest therapeutic potential for psychiatric indications** *Neuropsychopharmacology* **33**:685–700

Borenas M *et al.* (2021) **ALK ligand ALKAL2 potentiates MYCN-driven neuroblastoma in the absence of ALK mutation** *EMBO J* **40**

Brunet Avalos C, Maier GL, Bruggmann R, Sprecher SG (2019) **Single cell transcriptome atlas of the Drosophila larval brain** *Elife*

Cabrero P, Radford JC, Broderick KE, Costes L, Veenstra JA, Spana EP, Davies SA, Dow JA (2002) **The Dh gene of Drosophila melanogaster encodes a diuretic peptide that acts through cyclic AMP** *J Exp Biol* **205**:3799–3807

Cantera R, Nässel DR (1992) **Segmental peptidergic innervation of abdominal targets in larval and adult dipteran insects revealed with an antiserum against leucokinin I** *Cell Tissue Res* **269**:459–471

Cavanaugh DJ, Geratowski JD, Wooltorton JR, Spaethling JM, Hector CE, Zheng X, Johnson EC, Eberwine JH, Sehgal A (2014) **Identification of a circadian output circuit for rest:activity rhythms in Drosophila** *Cell* **157**:689–701

Cavey M, Collins B, Bertet C, Blau J (2016) **Circadian rhythms in neuronal activity propagate through output circuits** *Nat Neurosci* **19**:587–595

Cazes A *et al.* (2014) **Activated Alk triggers prolonged neurogenesis and Ret upregulation providing a therapeutic target in ALK-mutated neuroblastoma** *Oncotarget* **5**:2688–2702

Chen J, Reiher W, Hermann-Luibl C, Sellami A, Cognigni P, Kondo S, Helfrich-Forster C, Veenstra JA, Wegener C (2016) **Allatostatin A Signalling in Drosophila Regulates Feeding and Sleep and Is Modulated by PDF** *PLoS Genet* **12**

Cheng LY, Bailey AP, Leevers SJ, Ragan TJ, Driscoll PC, Gould AP (2011) **Anaplastic lymphoma kinase spares organ growth during nutrient restriction in Drosophila** *Cell* **146**:435–447

Chiu JC, Low KH, Pike DH, Yildirim E, Edery I (2010) **Assaying locomotor activity to study circadian rhythms and sleep parameters in Drosophila** *J Vis Exp*

Choksi SP, Southall TD, Bossing T, Edoff K, de Wit E, Fischer BE, van Steensel B, Micklem G, Brand AH (2006) **Prospero acts as a binary switch between self-renewal and differentiation in Drosophila neural stem cells** *Dev Cell* **11**:775–789

Cong X, Wang H, Liu Z, He C, An C, Zhao Z (2015) **Regulation of Sleep by Insulin-like Peptide System in Drosophila melanogaster** *Sleep* **38**:1075–1083

Crocker A, Guan XJ, Murphy CT, Murthy M (2016) **Cell-Type-Specific Transcriptome Analysis in the Mushroom Body Reveals Memory-Related Changes in Gene Expression** *Cell Reports* **15**:1580–1596

Davie K *et al.* (2018) **A Single-Cell Transcriptome Atlas of the Aging Drosophila Brain** *Cell* **174**:982–998

Donlea JM, Pimentel D, Talbot CB, Kempf A, Omoto JJ, Hartenstein V, Miesenbock G (2018) **Recurrent Circuitry for Balancing Sleep Need and Sleep** *Neuron* **97**:378–389

Dus M, Lai JS, Gunapala KM, Min S, Tayler TD, Hergarden AC, Geraud E, Joseph CM, Suh GS (2015) **Nutrient Sensor in the Brain Directs the Action of the Brain-Gut Axis in Drosophila** *Neuron* **87**:139–151

Englund C, Loren CE, Grabbe C, Varshney GK, Deleuil F, Hallberg B, Palmer RH (2003) **Jeb signals through the Alk receptor tyrosine kinase to drive visceral muscle fusion** *Nature* **425**:512–516

Gouzi JY, Moressis A, Walker JA, Apostolopoulou AA, Palmer RH, Bernards A, Skoulakis EM (2011) **The receptor tyrosine kinase Alk controls neurofibromin functions in Drosophila growth and learning** *PLoS Genet* **7**

Guo X, Yin C, Yang F, Zhang Y, Huang H, Wang J, Deng B, Cai T, Rao Y, Xi R (2019) **The Cellular Diversity and Transcription Factor Code of Drosophila Enteroendocrine Cells** *Cell Rep* **29**:4172–4185

Hart JE, Clarke IJ, Risbridger GP, Ferneyhough B, Vega-Hernandez M (2017) **Mysterious inhibitory cell regulator investigated and found likely to be secretogranin II related** *PeerJ* **5**

Helle KB (2004) **The granin family of uniquely acidic proteins of the diffuse neuroendocrine system: comparative and functional aspects** *Biol Rev Camb Philos Soc* **79**:769–794

Hewes RS, Park D, Gauthier SA, Schaefer AM, Taghert PH (2003) **The bHLH protein Dimmed controls neuroendocrine cell differentiation in Drosophila** *Development* **130**:1771–1781

Huckesfeld S *et al.* (2021) **Unveiling the sensory and interneuronal pathways of the neuroendocrine connectome in Drosophila** *Elife*

Imambocus BN *et al.* (2022) **A neuropeptidergic circuit gates selective escape behavior of Drosophila larvae** *Curr Biol* **32**:149–163

Inami S, Sato T, Sakai T (2022) **Circadian Neuropeptide-Expressing Clock Neurons as Regulators of Long-Term Memory: Molecular and Cellular Perspectives** *Front Mol Neurosci* **15**

Iwahara T, Fujimoto J, Wen D, Cupples R, Bucay N, Arakawa T, Mori S, Ratzkin B, Yamamoto T (1997) **Molecular characterization of ALK, a receptor tyrosine kinase expressed specifically in the nervous system** *Oncogene* **14**:439–449

Jin H, Stojnic R, Adryan B, Ozdemir A, Stathopoulos A, Frasch M (2013) **Genome-Wide Screens for Tinman Binding Sites Identify Cardiac Enhancers with Diverse Functional Architectures** *Plos Genetics*

Joiner WJ, Crocker A, White BH, Sehgal A (2006) **Sleep in Drosophila is regulated by adult mushroom bodies** *Nature* **441**:757–760

King AN, Barber AF, Smith AE, Dreyer AP, Sitaraman D, Nitabach MN, Cavanaugh DJ, Sehgal A (2017) **A Peptidergic Circuit Links the Circadian Clock to Locomotor Activity** *Curr Biol* **27**:1915–1927

Langmead B, Salzberg SL (2012) **Fast gapped-read alignment with Bowtie 2** *Nat Methods* **9**:357–359

Lasek AW, Gesch J, Giorgetti F, Kharazia V, Heberlein U (2011) **Alk is a transcriptional target of LMO4 and ERalpha that promotes cocaine sensitization and reward** *J Neurosci* **31**:14134–14141

Lasek AW *et al.* (2011) **An evolutionary conserved role for anaplastic lymphoma kinase in behavioral responses to ethanol** *PLoS One* **6**

Lee HH, Norris A, Weiss JB, Frasch M (2003) **Jelly belly protein activates the receptor tyrosine kinase Alk to specify visceral muscle pioneers** *Nature* **425**:507–512

Lewis JE, Brameld JM, Jethwa PH (2015) **Neuroendocrine Role for VGF** *Front Endocrinol (Lausanne)* **6**

Liao Y, Wang J, Jaehnig EJ, Shi Z, Zhang B (2019) **WebGestalt 2019: gene set analysis toolkit with revamped UIs and APIs** *Nucleic Acids Res* **47**:W199–W205

Liu W, Ganguly A, Huang J, Wang Y, Ni JD, Gurav AS, Aguilar MA, Montell C (2019) **Neuropeptide F regulates courtship in Drosophila through a male-specific neuronal circuit** *Elife*

Loren CE, Englund C, Grabbe C, Hallberg B, Hunter T, Palmer RH (2003) **A crucial role for the Anaplastic lymphoma kinase receptor tyrosine kinase in gut development in Drosophila melanogaster** *EMBO Rep* **4**:781–786

Lun AT, Smyth GK (2016) **csaw: a Bioconductor package for differential binding analysis of ChIP-seq data using sliding windows** *Nucleic Acids Res* **44**

Ma D, Przybylski D, Abruzzi KC, Schlichting M, Li Q, Long X, Rosbash M (2021) **A transcriptomic taxonomy of Drosophila circadian neurons around the clock** *Elife*

Maksimov DA, Laktionov PP, Belyakin SN (2016) **Data analysis algorithm for DamID-seq profiling of chromatin proteins in Drosophila melanogaster** *Chromosome Res* **24**:481–494

Marshall OJ, Brand AH (2017) **Chromatin state changes during neural development revealed by in vivo cell-type specific profiling** *Nat Commun* **8**

Matthay KK, Maris JM, Schleiermacher G, Nakagawara A, Mackall CL, Diller L, Weiss WA (2016) **Neuroblastoma** *Nature Reviews Disease Primers* **2**

Mendoza-Garcia P *et al.* (2021) **DamID transcriptional profiling identifies the Snail/Scratch transcription factor Kahuli as an Alk target in the Drosophila visceral mesoderm** *Development*

Mendoza-Garcia P *et al.* (2017) **The Zic family homologue Odd-paired regulates Alk expression in Drosophila** *PLoS Genet* **13**

Michki NS, Li Y, Sanjasaz K, Zhao Y, Shen FY, Walker LA, Cao W, Lee CY, Cai D (2021) **The molecular landscape of neural differentiation in the developing Drosophila brain revealed by targeted scRNA-seq and multi-informatic analysis** *Cell Rep* **35**

Nässel DR (2018) **Substrates for Neuronal Cotransmission With Neuropeptides and Small Molecule Neurotransmitters in Drosophila** *Front Cell Neurosci* **12**

Nässel DR, Zandawala M (2019) **Recent advances in neuropeptide signaling in Drosophila, from genes to physiology and behavior** *Prog Neurobiol* **179**

Nässel DR, Zandawala M (2022) **Endocrine cybernetics: neuropeptides as molecular switches in behavioural decisions** *Open Biol* **12**

Oh Y, Lai JS, Min S, Huang HW, Liberles SD, Ryoo HD, Suh GSB (2021) **Periphery signals generated by Piezo-mediated stomach stretch and Neuromedin-mediated glucose load regulate the Drosophila brain nutrient sensor** *Neuron* **109**:1979–1995

Okusawa S, Kohsaka H, Nose A (2014) **Serotonin and downstream leucokinin neurons modulate larval turning behavior in Drosophila** *J Neurosci* **34**:2544–2558

Orthofer M *et al.* (2020) **Identification of ALK in Thinness** *Cell* **181**:1246–1262

Pan X, O'Connor MB (2021) **Coordination among multiple receptor tyrosine kinase signals controls Drosophila developmental timing and body size** *Cell Rep* **36**

Park D, Veenstra JA, Park JH, Taghert PH (2008) **Mapping peptidergic cells in Drosophila: where DIMM fits in** *PLoS One* **3**

Pauls D, Chen J, Reiher W, Vanselow JT, Schlosser A, Kahnt J, Wegener C (2014) **Peptidomics and processing of regulatory peptides in the fruit fly Drosophila** *EuPA Open Proteomics* **3**:114–127

Pauls D, Hamarat Y, Trufasu L, Schendzielorz TM, Gramlich G, Kahnt J, Vanselow JT, Schlosser A, Wegener C (2019) **Drosophila carboxypeptidase D (SILVER) is a key enzyme in neuropeptide processing required to maintain locomotor activity levels and survival rate** *Eur J Neurosci* **50**:3502–3519

Pfeifer K, Wolfstetter G, Anthonydhason V, Masudi T, Arefin B, Bemark M, Mendoza-Garcia P, Palmer RH (2022) **Patient-associated mutations in Drosophila Alk perturb neuronal differentiation and promote survival** *Dis Model Mech*

Pitman JL, McGill JJ, Keegan KP, Allada R (2006) **A dynamic role for the mushroom bodies in promoting sleep in Drosophila** *Nature* **441**:753–756

Popichenko D *et al.* (2013) **Jeb/Alk signalling regulates the Lame duck GLI family transcription factor in the Drosophila visceral mesoderm** *Development* **140**:3156–3166

Quinlan AR (2014) **BEDTools: The Swiss-Army Tool for Genome Feature Analysis** *Curr Protoc Bioinformatics* **47**:11–34

Quinn JP, Kandigian SE, Trombetta BA, Arnold SE, Carlyle BC (2021) **VGF as a biomarker and therapeutic target in neurodegenerative and psychiatric diseases** *Brain Commun* **3**

Ramirez F, Dundar F, Diehl S, Gruning BA, Manke T (2014) **deepTools: a flexible platform for exploring deep-sequencing data** *Nucleic Acids Res* **42**:W187–191

Reim I, Hollfelder D, Ismat A, Frasch M (2012) **The FGF8-related signals Pyramus and Thisbe promote pathfinding, substrate adhesion, and survival of migrating longitudinal gut muscle founder cells** *Developmental Biology* **368**:28–43

Renn SC, Park JH, Rosbash M, Hall JC, Taghert PH (1999) **A pdf neuropeptide gene mutation and ablation of PDF neurons each cause severe abnormalities of behavioral circadian rhythms in Drosophila** *Cell* **99**:791–802

Reshetnyak AV, Murray PB, Shi X, Mo ES, Mohanty J, Tome F, Bai H, Gunel M, Lax I, Schlessinger J (2015) **Augmentor alpha and beta (FAM150) are ligands of the receptor tyrosine kinases ALK and LTK: Hierarchy and specificity of ligand-receptor interactions** *Proc Natl Acad Sci U S A* **112**:15862–15867

Rice P, Longden I, Bleasby A (2000) **EMBOSS: the European Molecular Biology Open Software Suite** *Trends Genet* **16**:276–277

Rohrbough J, Broadie K (2010) **Anterograde Jelly belly ligand to Alk receptor signaling at developing synapses is regulated by Mind the gap** *Development* **137**:3523–3533

Rohrbough J, Kent KS, Broadie K, Weiss JB (2013) **Jelly Belly trans-synaptic signaling to anaplastic lymphoma kinase regulates neurotransmission strength and synapse architecture** *Dev Neurobiol* **73**:189–208

Schaub C, Frasch M (2013) **Org-1 is required for the diversification of circular visceral muscle founder cells and normal midgut morphogenesis** *Dev Biol* **376**:245–259

Sellami A, Agricola HJ, Veenstra JA (2011) **Neuroendocrine cells in Drosophila melanogaster producing GPA2/GPB5, a hormone with homology to LH, FSH and TSH** *Gen Comp Endocrinol* **170**:582–588

Shafer OT, Keene AC (2021) **The Regulation of Drosophila Sleep** *Curr Biol* **31**:R38–R49

Shirinian M, Varshney G, Loren CE, Grabbe C, Palmer RH (2007) **Drosophila Anaplastic Lymphoma Kinase regulates Dpp signalling in the developing embryonic gut** *Differentiation* **75**:418–426

Southall TD, Gold KS, Egger B, Davidson CM, Caygill EE, Marshall OJ, Brand AH (2013) **Cell-type-specific profiling of gene expression and chromatin binding without cell isolation: assaying RNA Pol II occupancy in neural stem cells** *Dev Cell* **26**:101–112

Southey BR, Amare A, Zimmerman TA, Rodriguez-Zas SL, Sweedler JV (2006) **NeuroPred: a tool to predict cleavage sites in neuropeptide precursors and provide the masses of the resulting peptides** *Nucleic Acids Res* **34**:W267–272

Stay B, Chan KK, Woodhead AP (1992) **Allatostatin-immunoreactive neurons projecting to the corpora allata of adult Diploptera punctata** *Cell Tissue Res* **270**:15–23

Stuart T, Butler A, Hoffman P, Hafemeister C, Papalexi E, Mauck WM, Hao Y, Stoeckius M, Smibert P, Satija R (2019) **Comprehensive Integration of Single-Cell Data** *Cell* **177**:1888–1902

Stute C, Schimmelpfeng K, Renkawitz-Pohl R, Palmer RH, Holz A (2004) **Myoblast determination in the somatic and visceral mesoderm depends on Notch signalling as well as on milliways(mili(Alk)) as receptor for Jeb signalling** *Development* **131**:743–754

Sun LV, Chen L, Greil F, Negre N, Li TR, Cavalli G, Zhao H, Van Steensel B, White KP (2003) **Protein-DNA interaction mapping using genomic tiling path microarrays in Drosophila** *Proc Natl Acad Sci U S A* **100**:9428–9433

Takeda M, Suzuki T (2022) **Circadian and Neuroendocrine Basis of Photoperiodism Controlling Diapause in Insects and Mites: A Review** *Front Physiol* **13**

Tarasov A, Vilella AJ, Cuppen E, Nijman IJ, Prins P (2015) **Sambamba: fast processing of NGS alignment formats** *Bioinformatics (Oxford, England)* **31**:2032–2034

Torii S (2009) **Expression and function of IA-2 family proteins, unique neuroendocrine-specific protein-tyrosine phosphatases** *Endocr J* **56**:639–648

Tosti L, Ashmore J, Tan BSN, Carbone B, Mistri TK, Wilson V, Tomlinson SR, Kaji K (2018) **Mapping transcription factor occupancy using minimal numbers of cells in vitro and in vivo** *Genome Res* **28**:592–605

Uckun E, Wolfstetter G, Anthonydhason V, Sukumar SK, Umapathy G, Molander L, Fuchs J, Palmer RH (2021) **In vivo Profiling of the Alk Proximitome in the Developing Drosophila Brain** *J Mol Biol* **433**

Umapathy G, Mendoza-Garcia P, Hallberg B, Palmer RH (2019) **Targeting anaplastic lymphoma kinase in neuroblastoma** *APMIS*

Varshney GK, Palmer RH (2006) **The bHLH transcription factor Hand is regulated by Alk in the Drosophila embryonic gut** *Biochem Biophys Res Commun* **351**:839–846

Veenstra JA (2000) **Mono- and dibasic proteolytic cleavage sites in insect neuroendocrine peptide precursors** *Arch Insect Biochem Physiol* **43**:49–63

Veenstra JA, Agricola HJ, Sellami A (2008) **Regulatory peptides in fruit fly midgut** *Cell Tissue Res* **334**:499–516

Vernersson E, Khoo NK, Henriksson ML, Roos G, Palmer RH, Hallberg B (2006) **Characterization of the expression of the ALK receptor tyrosine kinase in mice** *Gene Expr Patterns* **6**:448–461

Vitzthum H, Homberg U, Agricola H (1996) **Distribution of Dip-allatostatin I-like immunoreactivity in the brain of the locust Schistocerca gregaria with detailed analysis of immunostaining in the central complex** *The Journal of comparative neurology* **369**:419–437

Wegener C, Gorbashov A (2008) **Molecular evolution of neuropeptides in the genus Drosophila** *Genome Biol* **9**

Weiss JB, Weber SJ, Torres ERS, Marzulla T, Raber J (2017) **Genetic inhibition of Anaplastic Lymphoma Kinase rescues cognitive impairments in Neurofibromatosis 1 mutant mice** *Behav Brain Res* **321**:148–156

Weiss JB, Xue C, Benice T, Xue L, Morris SW, Raber J (2012) **Anaplastic Lymphoma Kinase and Leukocyte Tyrosine Kinase: Functions and genetic interactions in learning, memory and adult neurogenesis** *Pharmacol Biochem Behav* **100**:566–574

Witek B, El Wakil A, Nord C, Ahlgren U, Eriksson M, Vernersson-Lindahl E, Helland A, Alexeyev OA, Hallberg B, Palmer RH (2015) **Targeted Disruption of ALK Reveals a Potential Role in Hypogonadotropic Hypogonadism** *PLoS One* **10**

Wolf FA, Angerer P, Theis FJ (2018) **SCANPY: large-scale single-cell gene expression data analysis** *Genome Biol* **19**

Wolfstetter G, Pfeifer K, van Dijk JR, Hugosson F, Lu X, Palmer RH (2017) **The scaffolding protein Cnk binds to the receptor tyrosine kinase Alk to promote visceral founder cell specification in Drosophila** *Science signaling*

Woodling NS *et al.* (2020) **The neuronal receptor tyrosine kinase Alk is a target for longevity** *Aging Cell* **19**

Wu F, Deng B, Xiao N, Wang T, Li Y, Wang R, Shi K, Luo DG, Rao Y, Zhou C (2020) **A neuropeptide regulates fighting behavior in Drosophila melanogaster** *Elife*

Yurgel ME, Kakad P, Zandawala M, Nässel DR, Godenschwege TA, Keene AC (2019) **A single pair of leucokinin neurons are modulated by feeding state and regulate sleep-metabolism interactions** *PLoS Biol* **17**

Zandawala M, Marley R, Davies SA, Nässel DR (2018) **Characterization of a set of abdominal neuroendocrine cells that regulate stress physiology using colocalized diuretic peptides in Drosophila** *Cell Mol Life Sci* **75**:1099–1115

Article and author information

Sanjay Kumar Sukumar

Department of Medical Biochemistry and Cell Biology, Institute of Biomedicine, University of Gothenburg, SE-405 30 Gothenburg, Sweden
ORCID iD: 0000-0001-9543-3113

Vimala Antonydhason

Department of Medical Biochemistry and Cell Biology, Institute of Biomedicine, University of Gothenburg, SE-405 30 Gothenburg, Sweden
ORCID iD: 0000-0001-6982-4030

Linnea Molander

Department of Medical Biochemistry and Cell Biology, Institute of Biomedicine, University of Gothenburg, SE-405 30 Gothenburg, Sweden
ORCID iD: 0009-0009-9266-1036

Jawdat Sandakly

Department of Experimental Pathology, Immunology and Microbiology, Faculty of Medicine, American University of Beirut, Beirut 1107 2020, Lebanon
ORCID iD: 0000-0002-5739-793X

Malak Kleit

Department of Experimental Pathology, Immunology and Microbiology, Faculty of Medicine, American University of Beirut, Beirut 1107 2020, Lebanon
ORCID iD: 0009-0004-2039-3507

Ganesh Umapathy

Department of Medical Biochemistry and Cell Biology, Institute of Biomedicine, University of Gothenburg, SE-405 30 Gothenburg, Sweden
ORCID iD: 0000-0003-2324-8300

Patricia Mendoza-Garcia

Department of Medical Biochemistry and Cell Biology, Institute of Biomedicine, University of Gothenburg, SE-405 30 Gothenburg, Sweden
ORCID iD: 0000-0002-6084-7962

Tafheem Masudi

Department of Medical Biochemistry and Cell Biology, Institute of Biomedicine, University of Gothenburg, SE-405 30 Gothenburg, Sweden
ORCID iD: 0000-0001-7406-9084

Andreas Schlossser

Julius-Maximilians-Universität Würzburg, Rudolf-Virchow-Center, Center for Integrative and Translational Bioimaging, 97080 Würzburg, Germany
ORCID iD: 0000-0003-0612-9932

Dick R. Nässel

Department of Zoology, Stockholm University, SE-106 91 Stockholm, Sweden
ORCID iD: 0000-0002-1147-7766

Christian Wegener

Julius-Maximilians-Universität Würzburg, Biocenter, Theodor-Boveri-Institute, Neurobiology and Genetics, 97074 Würzburg, Germany
ORCID iD: 0000-0003-4481-3567

Margret Shirinian

Department of Experimental Pathology, Immunology and Microbiology, Faculty of Medicine, American University of Beirut, Beirut 1107 2020, Lebanon
ORCID iD: 0000-0003-4666-2758

Ruth H. Palmer

Department of Medical Biochemistry and Cell Biology, Institute of Biomedicine, University of Gothenburg, SE-405 30 Gothenburg, Sweden
For correspondence: ruth.palmer@gu.se
ORCID iD: 0000-0002-2735-8470

Copyright

Editors

Reviewing Editor
Sonia Sen
Tata Institute for Genetics and Society, Bangalore, India

Senior Editor
K VijayRaghavan
National Centre for Biological Sciences, Tata Institute of Fundamental Research, Bangalore, India

Reviewer #2 (Public Review):

This manuscript illustrates the power of "combined" research, incorporating a range of tools, both old and new to answer a question. This thorough approach identifies a novel target in a well-established signalling pathway and characterises a new player in Drosophila CNS development.

Largely, the experiments are carried out with precision, meeting the aims of the project, and setting new targets for future research in the field. It was particularly refreshing to see the use of multi-omics data integration and Targeted DamID (TaDa) findings to triage scRNA-seq data. Some of the TaDa methodology was unorthodox, however, this does not affect the main finding of the study. The authors (in the revised manuscript) have appropriately justified their TaDa approaches and mentioned the caveats in the main text.

Their discovery of Spar as a neuropeptide precursor downstream of Alk is novel, as well as its ability to regulate activity and circadian clock function in the fly. Spar was just one of the downstream factors identified from this study, therefore, the potential impact goes beyond this one Alk downstream effector.

Reviewer #3 (Public Review):

Summary:

The receptor tyrosine kinase Anaplastic Lymphoma Kinase (ALK) in humans is nervous system expressed and plays an important role as an oncogene. A number of groups have been studying ALK signalling in flies to gain mechanistic insight into its various roles. In flies, ALK plays a critical role in development, particularly embryonic development and axon targeting. In addition, ALK also was also shown to regulate adult functions including sleep and memory. In this manuscript, Sukumar et al., used a suite of molecular techniques to identify downstream targets of ALK signalling. They first used targeted DamID, a technique that involves a DNA methylase to RNA polymerase II, so that GATC sites in close proximity to PolII binding sites are marked. They performed these experiments in wild type and ALK loss of function mutants (using an Alk dominant negative ALkDN), to identify Alk responsive loci. Comparing these loci with a larval single cell RNAseq dataset identified neuroendocrine cells as an important site of Alk action. They further combined these TaDa hits with data from RNA seq in Alk Loss and Gain of Function manipulations to identify a single novel target of Alk signalling - a neuropeptide precursor they named Sparkly (Spar) for its expression pattern. They generated a mutant allele of Spar, raised an antibody against Spar, and characterised its expression pattern and mutant behavioural phenotypes including defects in sleep and circadian function.

Strengths:

The molecular biology experiments using TaDa and RNAseq were elegant and very convincing. The authors identified a novel gene they named Spar. They also generated a mutant allele of Spar (using CrisprCas technology) and raised an antibody against Spar. These experiments are lovely, and the reagents will be useful to the community. The paper is also well written, and the figures are very nicely laid out making the manuscript a pleasure to read.

Weaknesses:

The manuscript has improved substantially in the revision. Yet, some concerns remain around the genetics and behavioural analysis which is incomplete and confusing. The authors generated a novel allele of Spar - Spar ΔExon1 and examined sleep and circadian phenotypes of this allele and of RNAi knockdown of Spar. The RNAi knockdown is a welcome addition. However, the authors only show one parental control the GAL4 / +, but leave out the other parental control i.e. the UAS RNAi / + e.g. in Fig. 9. It is important to show both parental controls.

Further, the sleep and circadian characterisation could be substantially improved. It is unclear how sleep was calculated - what program was used or what the criteria to define a sleep bout was. In the legend for Fig 8c, it says sleep was shown as "percentage of time flies spend sleeping measured every 5min across a 24h time span". Sleep in flies is (usually) defined as at least 5 min of inactivity. With this definition, I'm not sure how one can calculate the % time asleep in a 5 min bin! Typically people use 30min or 60min bins. The sleep numbers for controls also seem off to me e.g. in Fig. 8H and H' average sleep / day is ~100. Is this minutes of sleep? 100 min / day is far too low, is it a typo? The same applies to Figure 8, figure supplement 2. Other places e.g. Fig 8 figure supplement 1, avg sleep is around 1000 min / day. The numbers for sleep bouts are also too low to me e.g. in Fig 9 number of sleep bouts avg around 4, and in Fig. 8 figure supplement 2 they average 1 sleep bout. There are several free software packages to analyse sleep data (e.g. Sleep Mat, PMID 35998317, or SCAMP). I

would recommend that the authors reanalyse their data using one of these standard packages that are used routinely in the field. That should help resolve many issues.

The circadian anticipatory activity analyses could also be improved. The standard in the field is to perform eduction analyses and quantify anticipatory activity e.g. using the method of Harrisingh et al. (PMID: 18003827). This typically computed as the ratio of activity in the 3hrs preceding light transition to activity in the 6hrs preceding light transition. The programs referenced above should help with this.

Finally, in many cases I'm not sure that the appropriate statistical tests have been used e.g. in Fig 8c, 8e, 8h t-tests have been used when are three groups in the figure. The appropriate test here would an ANOVA, followed by post-hoc comparisons.

- https://doi.org/10.7554/eLife.88985.2.sa0

Author Response

The following is the authors' response to the original reviews.

> *eLife assessment*
>
> *Receptor tyrosine kinases such as ALK play critical roles during appropriate development and behaviour and are nodal in many disease conditions, through molecular mechanisms that weren't completely understood. This manuscript identifies a previously unknown neuropeptide precursor as a downstream transcriptional target of Alk signalling in Clock neurons in the Drosophila brain. The experiments are well designed with attention to detail, the data are solid and the findings will be useful to those interested in events downstream of signalling by receptor tyrosine kinases.*

Authors response: We thank the reviewers for this assessment of our Manuscript. We are happy to accept the current eLife assessment of our manuscript. In our revised manuscript we have addressed all of the major reviewer comments, including additional experiments suggested by the reviewers, which have significantly strengthened the revised version.

> *Reviewer #1 (Public Review):*
>
> *Sukumar et al build on a body of work from the Palmer lab that seeks to unravel the transcriptional targets of Alk signaling (a receptor tyrosine kinase). Having uncovered its targets in the mesoderm in an earlier study, they seek to determine its targets in the central nervous system. To do this, they use Targeted DamID (TaDa) in the wild-type and Alk dominant negative background and identify about 1700 genes that might be under the control of Alk signalling. Using their earlier data and applying a set of criteria - upregulated in gain-of-Alk, downregulated in loss-of-Alk, and co-expressed with Alk positive cells in single cell datasets - they arrive upon a single gene, Sparkly, which is predicted to be a neuropeptide precursor.*
>
> *They generate antibodies and mutants for Sparkly and determine that it is responsive to Alk signalling and is expressed in many neuroendocrine cells, as well as in clock neurons. Though the mutants survive, they have reduced lifespans and are hyperactive. In summary, the authors identify a previously unidentified transcriptional target of Alk signalling, which is likely cleaved into a neuropeptide and is involved in regulating circadian activity.*
>
> *The data support claims made, are generally well presented and the manuscript clearly written. The link between circadian control of Alk signalling in Clock neurons > Spar expression > ultimately controlling circadian activity, however, was not clear.*

Authors response: We thank the reviewer for this through reading of our manuscript and for kindly highlighting the important takeaways from the study. The role of Alk signalling in activity, circadian rhythm and sleep has previously been reported by other groups in the following studies – (Bai and Sehgal, 2015; Weiss et al, 2017; Gouzi, Bouraimi et al 2018), which we have discussed in our manuscript. We also have identified a hyperactivity phenotype in our Alk CNS specific loss-of-function allele, AlkRA, which is similar to the Spar loss-of-function mutant phenotype. We hypothesize that one of ways in which Alk signalling regulates fly activity is through regulating Spar gene expression in neuroendocrine cells. This is supported by our data which shows Alk expression in Clock neurons, as well by the new experimental data showing an activity phenotype in flies expressing Spar RNAi driven by the Clk678-Gal4 driver.

> **Reviewer #2 (Public Review):**
>
> *This manuscript illustrates the power of "combined" research, incorporating a range of tools, both old and new to answer a question. This thorough approach identifies a novel target in a well-established signalling pathway and characterises a new player in Drosophila CNS development.*
>
> *Largely, the experiments are carried out with precision, meeting the aims of the project, and setting new targets for future research in the field. It was particularly refreshing to see the use of multi-omics data integration and Targeted DamID (TaDa) findings to triage scRNA-seq data. Some of the TaDa methodology was unorthodox (and should be justifed/caveats mentioned in the main text), however, this does not affect the main finding of the study.*
>
> *Their discovery of Spar as a neuropeptide precursor downstream of Alk is novel, as well as its ability to regulate activity and circadian clock function in the fly. Spar was just one of the downstream factors identified from this study, therefore, the potential impact goes beyond this one Alk downstream effector.*

Authors response: We thank the reviewer for the positive comments highlighting the strengths of our study. TaDa was used as a semi-quantitative readout of the transcriptional activity in a Alk loss-of-function background with an emphasis on relative differences in peaks close to GATC sites, providing an important dataset for integration with bulk and single cell RNAseq. As the reviewer points out there are important considerations when interpreting this data and we have now added sentences in the discussion to inform readers of possible caveats of our TaDa dataset.

> **Reviewer #3 (Public Review):**
>
> *Summary:*
>
> *The receptor tyrosine kinase Anaplastic Lymphoma Kinase (ALK) in humans is nervous system expressed and plays an important role as an oncogene. A number of groups have been signalling ALK signalling in flies to gain mechanistic insight into its various role. In flies, ALK plays a critical role in development, particularly embryonic development and axon targeting. In addition, ALK also was also shown to regulate adult functions including sleep and memory. In this manuscript, Sukumar et al., used a suite of molecular techniques to identify downstream targets of ALK signalling. They first used targeted DamID, a technique that involves a DNA methylase to RNA polymerase II, so that GATC sites in close proximity to PolII binding sites are marked. They performed these experiments in wild-type and ALK loss of function mutants (using an Alk dominant negative ALkDN), to identify Alk responsive loci. Comparing these loci with a larval single-cell RNAseq dataset identified neuroendocrine cells as an important site of Alk action.*

They further combined these TaDa hits with data from RNA seq in Alk Loss and Gain of Function manipulations to identify a single novel target of Alk signalling - a neuropeptide precursor they named Sparkly (Spar) for its expression pattern. They generated a mutant allele of Spar, raised an antibody against Spar, and characterised its expression pattern and mutant behavioural phenotypes including defects in sleep and circadian function.

Strengths:

The molecular biology experiments using TaDa and RNAseq were elegant and very convincing. The authors identified a novel gene they named Spar. They also generated a mutant allele of Spar (using CrisprCas technology) and raised an antibody against Spar. These experiments are lovely, and the reagents will be useful to the community. The paper is also well written, and the figures are very nicely laid out making the manuscript a pleasure to read.

Weaknesses:

My main concerns were around the genetics and behavioural characterisation which is incomplete. The authors generated a novel allele of Spar - Spar ΔExon1 and examined sleep and circadian phenotypes of this allele. However, they have only one mutant allele of Spar, and it doesn't appear as if this mutant was outcrossed, making it very difficult to rule out off-target effects. To make this data convincing, it would be better if the authors had a second allele, perhaps they could try RNAi?

Further, the sleep and circadian characterisation could be substantially improved. In Fig 8 E-F it appears as if sleep was averaged over 30 days! This is a little bizarre. They then bin the data as day 1 - 12 and 12-30. This is not terribly helpful either. Sleep in flies, as in humans, undergoes ontogenetic changes - sleep is high in young flies, stabilises between day 3-12, and shows defects by around 3 weeks of age (cf Shaw et al., 2000 PMID 10710313). The standard in the sleep field is to average over 3 days or show one representative day. The authors should reanalyse their data as per this standard, and perhaps show data from 310 day old flies, and if they like from 20-30 day old flies. Further, sleep data is usually analysed and presented from lights on to lights on. This allows one to quantify important metrics of sleep consolidation including bout lengths in day and night, and sleep latency. These metrics are of great interest to the community and should be included.

The authors also claim there are defects in circadian anticipatory activity. However, these data, as presented are not solid to me. The standard in the field is to perform eduction analyses and quantify anticipatory activity e.g. using the method of Harrisingh et al. (PMID: 18003827). Further, circadian period could also be evaluated. There are several free software packages to perform these analyses so it should not be hard to do.

Authors response: We thank the reviewer for the thorough reading of our manuscript and for generously praising the positives as well as pointing out the weakness of our study. We have now addressed the highlighted weaknesses in behavioural experiments. In particular, we have reanalysed our data according to the reviewer's suggestions. In addition, we provide experimental data, driving Spar RNAi in Clock neurons, that support our Spar mutant analysis.

Point-by-point response to the reviewers' concerns:

Point 1. "My main concerns were around the genetics and behavioural characterisation which is incomplete. The authors generated a novel allele of Spar - Spar ΔExon1 and examined sleep and circadian phenotypes of this allele. However, they have only one mutant allele of Spar, and it doesn't appear as if this mutant was outcrossed, making it

very difficult to rule out off-target effects. To make this data convincing, it would be better if the authors had a second allele, perhaps they could try RNAi?"

Authors response: As per the reviewer's suggestion, we conducted a targeted knockdown of Sparkly specifically in clock neurons (Clk-Gal4 > Spar-RNAi) and assessed the circadian phenotypes. Flies were monitored for 5 days in LD followed by a shift to DD, similar to our previous LD-DD experiments. The results revealed a significant disruption in both activity and sleep during the DD transition period upon knockdown of Spar in circadian clock neurons. These findings strongly align with the expression pattern of Spar in clock neurons (Figure 7i-l"). We have now included a new main figure (Figure 9) together with several supplementary figure (Figure 9 – figure supplements 1 and 2) and discussed these experiments on pages 17-18 of the results section of the revised manuscript.

Point 2. "Further, the sleep and circadian characterisation could be substantially improved. In Fig 8 E-F it appears as if sleep was averaged over 30 days! This is a little bizarre. They then bin the data as day 1 - 12 and 12-30. This is not terribly helpful either. Sleep in flies, as in humans, undergoes ontogenetic changes - sleep is high in young flies, stabilises between day 3-12, and shows defects by around 3 weeks of age (cf Shaw et al., 2000 PMID 10710313). The standard in the sleep field is to average over 3 days or show one representative day. The authors should reanalyse their data as per this standard, and perhaps show data from 3–10-day old flies, and if they like from 20–30-day old flies."

Authors response: We have reanalysed these data according to the reviewer's suggestions and revised the sleep data presented. Specifically, we have focused on two 3-day periods, days 5-7 as well as days 20-22. By averaging the sleep mean during these time points, we observed a significant decrease in average sleep duration in the SparΔExon1 and Alk ΔRA mutant flies at a younger age (Figure 8h-h', Figure 8 – figure supplement 2). However, no significant effect was observed in older flies (Figure 8h-h', Figure 8 – figure supplement 2). We have incorporated this new data into Figure 8 and provided a detailed description in the results section (page 16) of the revised manuscript.

Point 3. "Further, sleep data is usually analysed and presented from lights on to lights on. This allows one to quantify important metrics of sleep consolidation including bout lengths in day and night, and sleep latency. These metrics are of great interest to the community and should be included."

Authors response: We have now reanalysed these data as per the reviewer's suggestion. From the raw data collected over a span of 3 days, we specifically selected the lights on-lights on data and examined the average sleep duration. Notably, we observed a significant downregulation of average sleep in SparΔExon1 and AlkΔRA flies, but only at a younger age (Figure 8h-h', Figure 8 – figure supplement 2). Furthermore, we assessed the number of sleep bouts using this data and found a significant increase in the number of bouts in younger SparΔExon1 and AlkΔRA flies, with no changes observed at an older age (Figure 8 – figure supplement 2). Additionally, we evaluated the number of bouts in flies that were initially monitored in LD and then shifted to DD, observing a significant decrease in the number of sleep bouts in SparΔExon1 flies following the transition to DD (Figure 9d). This new data is described in detail in the results section (pages 16-18) of the revised manuscript.

Point 4. "The authors also claim there are defects in circadian anticipatory activity. However, these data, as presented are not solid to me. The standard in the field is to perform eduction analyses and quantify anticipatory activity e.g. using the method of Harrisingh et al. (PMID: 18003827)."

Authors response: We appreciate the valuable suggestion provided by the reviewer. In accordance with the referenced paper by Harrisingh et al. (2007), we calculated the "anticipation score" defined as the percentage of activity in the 6hour period preceding the lights-on or lights-off transition that occurs in the 3-hour window just before the transition. To analyse the mean activity of the flies, we selected the data corresponding to the 6 hours before lights-on and the 6 hours before lights-off, averaged over a 14-day period under normal LD conditions. Interestingly, we observed a significant increase in the mean activity of SparΔExon1 flies during both morning anticipation (a.m. anticipation) and evening anticipation (p.m. anticipation) (Figures 8f). Furthermore, we analysed this parameter for flies entrained in DD and found that SparΔExon1 flies exhibited lower mean activity during both morning and evening anticipation (Figures 8g). We have incorporated this new data into Figure 8 and provided a detailed description in the results section (pages 16-18) of the revised manuscript.

> *Point 5. Further, circadian period could also be evaluated. There are several free software packages to perform these analyses so it should not be hard to do.*

Authors response: We have now evaluated the circadian period as suggested by the reviewer; generating a chi-square periodogram for each fly to calculate the free-running period for the flies that were under normal LD conditions additionally to the ones that were entrained in DD. We calculated the percentage of flies that had a shorter or longer period than 1440 min (24 h) and observed that w1118 and SparΔExon1 flies have a longer circadian period (Figure 8 – figure supplement 4) but following the shift to DD, they tend to have a shorter circadian period (Figure 9 – figure supplement 3). This new data is described in the results (pages 16-18).

> ***Recommendations for the authors:***
>
> *There are two major concerns that we recommend the authors address:*
>
> 1. *The behaviour: There are a number of unconventional representations of the behavioural data in this manuscript. We recommend that the authors revisit their data representation to adhere to conventions in the field - specific suggestions are in the reviews. We also suggest an additional experiment - an RNAi/different allele/rescue experiment to ensure that the phenotypes the authors observe are not due to off-target effects of the mutant they have generated.*

Authors response: In the revised manuscript, we have reanalysed the behavioural data according to the reviewers' recommendations (included in Figures 8 and 9 of the revised version). In addition, we have performed a targeted Spar RNAi experiment in clock neurons (included in Figure 9 of the revised version), identifying a hyperactive behavioural phenotype similar to that of Spar mutants. The inclusion of these new analyses and data strengthens the manuscript and support the conclusion that Spar plays a role in regulation of behaviour.

> 1. *TaDa analyses: We were concerned that the authors might be picking up false positives with the way they have analysed their data. While this may not matter for this study, it will be useful to reason out their approach and keep this in mind for any other targets they choose from these data for further studies.*

Authors response: In line with the reviewers concerns we have now highlighted the potential caveats and drawbacks of our TaDa dataset in the discussion section of the revised manuscript (detailed in response to Reviewer #2 below).

Reviewer #1 (Recommendations For The Authors):

Though generally well written, I felt that some sections could be written in more detail. For example, the text around Figure 5 was not very informative. Many of the other approaches to the analyses and details of datasets used were glossed over. Since the manuscript uses a lot of previously published data, it would be nice to give more details about them in the context of the results.

Authors response: We thank the reviewer for this recommendation. We have now added additional information about peptidomics analysis in the results and in the legend of Figure 5. We have also included a table in the Methods that summarised the datasets used in this study, including the Dataset name, brief description and reference.

In the panels where co-localisations have been represented, it would be nice to include enlarged insets depicting the co-labelling. It is not always obvious in the way the figures have currently been represented. For example, in Fig 2G, Alk stain appears to be everywhere, but the authors make the point that it is enriched in neuroendocrine cells (as labelled by dimmed), but the co-localisation isn't evident. Similar issues come up with the sparkly colocalisations.

Authors response: As suggested by the reviewer, we have now added additional panels to complement the stainings in Figure 2G. These new data are included as Figure 2 – figure supplement 1 (Alk/Dimm-Gal4>UAS-GFPcaax staining) and as Figure 4 – figure supplement 1 (Alk/Spar staining), which indicate colocalization in the central brain and ventral nerve cord prosecretory cells with enlarged panels.

Supplementary figures S3C and 3F appear garbled to me? Maybe it didn't upload properly?

Authors response: Unfortunately, this issue is not apparent to us. However, we have now re-uploaded these Figures.

Sparkly's responsiveness to Alk signalling: Visually, there does not seem to be an increase or decrease in spar levels in the images in Fig 4F-H. How was the quantification done? I would suggest a more detailed interpretation of their results related to spar's responsiveness to Alk signalling - at the mRNA vs protein levels and the GOF vs LOF conditions.

Authors response: We thank the reviewer for this constructive recommendation. In the revised manuscript, we have now repeated this experiment with increased numbers of larval CNS followed by blinded image analysis. These results also show an increased fluorescence intensity as measured by corrected total cell fluorescence (CTCF), confirming our previous observation of increased Spar protein expression in in Alk gain-of-function conditions compared to controls. In this analysis, changed in Spar levels in Alk loss-of-function remained non-significant compared to control, in agreement with our previous data. As suggested by the reviewer, we have now included several additional sentences discussing the possible reasons for these observations. This following text is now included on Page 11 of the results section:

"While our bulk RNA-seq and TaDa datasets show a reduction in Spar transcript levels in Alk loss-of-function conditions, this reduction is not reflected at the protein level. This observation may reflect additional uncharacterised pathways that regulate Spar mRNA levels as well as translation and protein stability. Taken together, these observations confirm that Spar expression is responsive to Alk signaling in CNS, although Alk is not critically required

to maintain Spar protein levels." We have also added an additional Image analysis method section explaining the methodology of the CTCF fluorescent intensity quantification on Page 28.

> **Reviewer #2 (Recommendations For The Authors):**
>
> *It was surprising to see that the authors did not use Dam-only controls. This is to control for background methylation by Dam (i.e. accessible chromatin). This does not invalidate the main results of the manuscript, however, there could be false positives in the dataset for genes that are seen to be up-regulated in the mutant condition (e.g. if accessibility is increased in the mutant but not transcription, then it would look like increased Pol II binding, when it isn't). As the study was focusing on genes down-regulated in the mutant, this is less of an issue, as it is very unlikely to see an increase in transcription with a decrease in accessibility (that could provide a false positive). The authors should explain their rationale for not using Dam-only controls, and the associated caveats, in the manuscript.*

Authors response: We agree with the reviewer's comment on possibility of identifying false positive candidates from our TaDa dataset. Especially, if one is seeking to find a gene with increased Pol II occupancy in a Alk dominant negative condition. However, our analysis only focuses on genes which are responsive to Alk-manipulation, namely, genes which are downregulated in the Alk dominant negative condition. One of the rationales for not using a Dam-only control was that in our previous Mendoza-Garcia et al, 2021 study, we employed a similar method and were able to successfully identify already known and novel targets of Alk signalling in embryonic mesoderm comparing the Dam-Pol II versus Dam-Pol II; Alk Dominant negative conditions. In the current version of the manuscript, we have expanded our discussion of these caveats as follows (Discussion, Page 19-20):

"A potential drawback of our TaDa dataset is the identification of false positives, due to non-specific methylation of GATC sites at accessible regions in the genome by Dam protein. Hence, our experimental approach likely more reliably identifies candidates which are downregulated upon Alk inhibition. In our analysis, we have limited this drawback by focusing on genes downregulated upon Alk inhibition and integrating our analysis with additional datasets, followed by experimental validation. This approach is supported by the identification of numerous previously iden- tied Alk targets in our TaDa candidate list."

> *Related to this, could the authors make it clear/justify why they chose to use peakbased analysis of the Dam-Pol II data rather than looking at signals across whole transcripts? For example, this could result in false positives if a gene switches from having no Pol II to having paused Pol II.*

Authors response: In our opinion, a peak based analysis is dependable in this context. We chose to prioritize peaks close (+/- 1kb) to transcription start sites (TSS) to increase the chances of finding true Pol II occupancy peaks. Also, during bioinformatics analysis using Damid-seq pipeline (Maksimov et al, 2016) fragments not aligning to GATC borders are excluded. Therefore, a whole transcript Pol II occupancy peak analysis may not be always feasible. We agree with the reviewer that a paused Pol II will result in false positives, however, it will only result in an increase of a specific peak and in our case, we are seeking to identify peaks with lower pol II occupancy as a result of Alk knockdown. Furthermore, we depend on additional integration with additional relevant datasets to minimise false positive candidates for detailed analysis. In the current version of the manuscript these caveats have been mentioned and discussed (see point above).

> *Do the authors have any theories about the mode of action of Spar? Or ideas about how this might be followed up? If so, that could be included in the Discussion.*

Authors response: Other than identifying modified Spar derived peptides, which suggest a target receptor, possibly a GPCR, were have no other data currently that allows us to speculate more on the mode of action of Spar. We are currently working hard to try to identify a receptor, but this is a challenging and ongoing process. In the discussion we speculate regarding the identity of the Spar receptor, as well as its location, which is likely in the CNS, and body muscle, however, these are open questions that we can hopefully answer in a future study.

> ***Reviewer #3 (Recommendations For The Authors):***
>
> *Spar protein expression was unchanged in Alk loss of function. This is a curious result as the authors used RNA seq data from Alk loss of function to identify Spar. This could be commented on in the discussion.*

Authors response: We thank the reviewer for this comment, and they are correct in noticing this. We have also thought about this, and reviewer #1 also commented. To confirm this result, we repeated this experiment with increased numbers of larval CNS followed by blinded image analysis for the revised version. These results also show an increased fluorescence intensity as measured by corrected total cell fluorescence (CTCF), confirming our previous observation of increased Spar protein expression in in Alk gain-of-function conditions compared to controls. In this analysis, changed in Spar levels in Alk loss-of-function remained non-significant compared to control, in agreement with our previous data. As suggested by reviewer #1, we have now included several additional sentences discussing the possible reasons for these observations. This following text is now included on Page 11 of the results section:

"While our bulk RNA-seq and TaDa datasets show a reduction in Spar transcript levels in Alk loss-of-function conditions, this reduction is not reflected at the protein level. This observation may reflect additional uncharacterised pathways that regulate Spar mRNA levels as well as translation and protein stability. Taken together, these observations confirm that Spar expression is responsive to Alk signaling in CNS, although Alk is not critically required to maintain Spar protein levels."

> *Pg 19: Spar is expressed in the Mushroom Bodies (MBs). Do they mean in Kenyon Cells (KCs)? I don't see this expression in the figures. Maybe this could be highlighted in the figure. It would definitely be of interest if this were true.*

Authors response: We agree with the reviewer that this would be interesting. We have not performed detailed staining of the mushroom bodies at this point, however, Spar mRNA expression in a transcriptomics analysis performed by Crocker et al, 2016, identifies Spar in all cell types, including Kenyon cells. We have now included this and cited this reference in the discussion.

> *Spar is also expressed in multiple potential sleep regulatory sites including clock neurons, the PI, AstA cells and so on. Some of these might be arousal-promoting and some sleep-promoting. Taking out Spar in both sleep and arousal-promoting subsets might have complex effects. The authors might want to knock down Alk in different subsets of neurons to make more targeted manipulations.*

Authors response: We thank the reviewer for this suggestion regarding interesting experiments to further investigate Spar function. We are planning to follow up and study the role of Alk signalling in different neuronal subsets, with a specific interest in neuroendocrine/prosecretory cells.